Cement and Concrete Research 192 (2025) 107854

Contents lists available at ScienceDirect

Cement and Concrete Research

journal homepage: www.elsevier.com/locate/cemconres

# From bauxite residue mineralogy to reactivity and properties of blended cements

Michael Wenzel *, Fabien Georget, Thomas Matschei

*Institute for Construction Materials Research (IBAC), RWTH Aachen University, Schinkelstraße 3, 52062 Aachen, Germany*

ARTICLE INFO

*Keywords:*
Bauxite residue mineralogy
Activation of bauxite residue
Durability of bauxite residue blended cements
Reactivity of bauxite residue
Properties of bauxite residue blended cements

ABSTRACT

This paper reviews the efforts taken towards developing bauxite residue (BR) based blended cements (>30% substitution) contributing to the cement industry's net-zero targets, while utilizing the Bayer-processes by-product. We provide a comprehensive review of physical properties, element composition and mineralogy of Bayer and sintering BR. This defines the main challenges that BR based SCMs have to overcome to be utilized in sustainable blended cements. Several activation treatments and their impact on SCM characteristics and reactivity are introduced and compared to other reactive SCMs.

Furthermore, the review summarizes the impact of BR addition on the engineering performance of blended cements and includes selected durability issues. Our main goal is linking macroscopic observations to microstructural features of the binders and outlining a way towards a complete understanding of these blended cements. We outline specific knowledge gaps, in particular the effect of bauxite residues on the phase assemblage and microstructure of blended cements.

## 1. Introduction

### 1.1. Context and objectives

The cement production emits approx. 2.2 Gt $CO_2$/year, which equals 6% of the global GHG emission in 2017 [1]. During clinker burning 35% of the total emissions are generated through fuel combustion, while the calcination of limestone (process intrinsic emission) amounts to approx. 55% of the carbon footprint of OPC [2–5]. Therefore, several strategies have been developed to reduce the environmental impact of Portland clinker-based cements [6,7]. One approach is the development of alternative binder and clinker concepts as well as the use of supplementary cementitious materials (SCMs).

Currently ground granulated blast furnace slag (GGBFS) and silicon-rich fly ash (FA) are the main SCMs used in cementitious systems. The increasing SCM demand of the cement industry, and the shift of steel and energy production towards more sustainable production technologies, makes the exploitation of new SCM sources an urgent industrial objective. This leads to a renewed research interest in natural pozzolans like volcanic ashes [8–10], trass [11], calcined clays [12,13] and unused industrial wastes like copper tailings [14,15] or, the subject of this review, bauxite residue (BR) [16–19].

BR is the alkaline waste of primary alumina production, which increased from 42,183 kt alumina in 1993 to 143,313 kt in 2023 [20,21]. The annual BR production rose from 150 Mio.t/a [17] to 175 Mio.t/a between 2016 and 2019 [22]. The legacy BR (estimates 7 to 8 billion tonnes) is one of the alumina industries main sustainability problems.

Its main issue is the long-term storage, which causes environmental risks (contamination of phreatic waters, as well as dust emissions) and maintenance efforts. Due to the strategic location of large alumina plants in rural areas in e.g. India or Brazil the economic pressure for BR utilization is (currently) not very strong.

A complete reuse of BR is only possible through large material streams. The most promising options are construction materials and soil beneficiation. While 180 Mt/a are not comparable to the global production of fly ash (700 to 1100 Mt/a) or GGBFS (300 to 360 Mt/a) they are significant on a local scale [23]. To take a decisive step towards a circular alumina industry BR valorisation is of high importance, which led to dedicated technological roadmaps e.g. from the International Alumina Institute [24], whose success would contribute to the aluminium industries net zero policy [25,27]. Table 1 showcases that BR is a significant waste stream comparable to e.g. type C fly ashes, while not being as available as bio ashes and some other pozzolanic SCMs. It

* Corresponding author.
*E-mail addresses:* wenzel@ibac.rwth-aachen.de (M. Wenzel), georget@ibac.rwth-aachen.de (F. Georget), matschei@ibac.rwth-aachen.de (T. Matschei).

https://doi.org/10.1016/j.cemconres.2025.107854
Received 25 June 2024; Received in revised form 6 December 2024; Accepted 25 February 2025
Available online 3 March 2025

**Table 1**
Impression of global production of selected SCMs in Mt/a.

| SCM type | Annual production Mt | Year | Source |
|---|---|---|---|
| Fly ash C | 100 to 200 | 2016 | [26] |
| Fly ash F | 600 to 900 | 2016 | |
| GGBSF | 300 to 360 | 2016 | |
| Bio ash (FA F equivalent) | 100–140 | 2016 | [26] |
| Copper slag | 30–40 | 2016 | |
| Silica fume | 1 to 2.5 | 2016 | |
| Bauxite residue | 150 to 180 | 2019 | [22] |
| Natural pozzolans | 75 (most likely large untapped reserves) | 2016 | [26] |
| Rice husk ash | Approx. 30 | 2017 | [28] |
| Limestone | 300 | 2016 | [26] |

should be pointed out that the given data should only be taken as estimates, since an in-depth review of promising SCM material streams is besides the scope of this paper.

While BR is not able to replace SCMs like fly ash type F the produced amounts and legacy volumes are large enough to justify a standardization effort for BR blended cements.

Because of the cement industries huge material streams the raw material and SCM supply remain on a regional level. This makes BR based blended cements a valid option for countries like Greece, Brazil or India. In this context high replacement levels are needed to pique the interest of the cement industry, because they need to reduce clinker factors (CFs) below 0.7 to reach their sustainability goals. BR has unique properties. A pozzolanic reactivity of BRs was demonstrated [18]. However, its reactivity is comparatively low because significant amounts of alumina are immobilized in inert crystalline phases. In addition, environmental compatibility and sodium contents are considered critical issues [29,30]. This explains, why BR utilization in the cement industry is currently restricted to low replacement levels and local applications, like the utilization of 2 Mt/a in 40 Indian cement plants [31].

The need for BR utilization initiated projects like RemovAl (H2020 grant agreement 776469) or ReActiv (H2020 grant agreement 958208) to investigate BR as a component of geopolymers [32,33], CSA cements [34] and SCMs. Activation treatments based on calcination and vitrification processes were developed to enhance the BR's reactivity in blended cements [35–37]. The results indicate that the sodium content of BR is not necessarily detrimental for the application of 10–30 wt% BR in blended cements [36,38,39]. However, the BR's impact on phase assemblage, porosity, and hence durability properties and strength evolution is not sufficiently understood. The potential of BR as an aluminate-rich SCM, and the impact of its mineralogy on the interaction with the cementitious system, remain unclear.

In this review, the properties of BR containing blended cements are related to the composition and mineralogy of BR. When necessary the published data are complemented by some of our own investigations. Furthermore, modified BR, and the corresponding activation technologies are presented. The impact of BR, and BR-based SCMs on the properties of concretes will be reviewed. Finally, we want to give an outlook on the impact of BR addition on concrete durability. One objective of this review is to point out knowledge gaps regarding microstructural understanding and macroscopic performance of BR-blended cements. We restrict our discussions to the main elements participating in the formation of hydrates in a cementitious system. As such, although an important topic for widespread use of these materials, the potential environmental compatibility issues due to the heavy metals will not be discussed in depth [40,41].

### 1.2. Methodology

The methodology used to extract and discuss quantitative values from literature needs to be briefly outlined. The search for publications was carried out using GoogleScholar and WebofScience. The utilized search phrases are documented in the supplementary material (Keywords.xls) arranged in order of the paper's main sections. The selection of sources occurred by manual sampling of abstracts and conclusions. Due to the low number of datasets (<30 replicates per data points) no advanced statistics were used to analyse the data. Error bars were taken from the source publications, if these did not calculate standard deviations despite having at least 3 replicates, the scatter is given as the 1 σ quantile of the scientific standard deviation. If that is not possible no scatter is given. The collected raw data are tabulated and linked to the sources in the supplementary materials, since in this paper the focus is set on trends and correlations instead of significant, quantitative values.

## 2. Processes for primary aluminium production

Alumina can be produced from the bauxite ores via two routes: the Bayer and the soda sintering process. With only a few remaining plants, the latter is being progressively substituted by the Bayer process. These processes are summarized in Fig. 1. As the Bayer route makes up approximately 95% of the currently produced BR, this review, and most current research, focus on Bayer BRs [17,42]. Basic information on the sintering process and the application of soda-sintering BRs are included for completeness.

### 2.1. The Bayer process

Lateral[1] and karstic[2] bauxites with high Al/Si ratios are processed through the Bayer process [14,44,45,49]. Diasporic[3] and other bauxites with quartz or clay impurities (kaolinites/muscovites, etc.) have to be treated with pre-desilication steps (the addition of lime suspension) before they can be digested. The most silica-rich bauxites used in this process contain up to 70 wt% of diaspore and clay phases [51]. The Bayer process is adapted to the parent ore (e.g. boemitic, gibbsitic, or diasporic bauxite), leading to different plant designs [44–47].

A simplified process is shown in Fig. 1a). The parent ore is ground in a Na(OH) slurry and then leached at elevated temperature (100–250 °C). The digestion mainly dissolves gibbsite, boehmite, or diaspore present in the ore. Clay minerals release significant amounts of silicate into the green liquor, while the iron-rich phases remain inert.

The silicates precipitate during the clarification step as the desilication product (DSP). This is necessary to ensure the purity of the alumina. Then the solid BR is separated from the green liquor, which contains $Al(OH)_4^-$. Additional washing steps and filter pressing reduce the amount of Na(OH) in the BR. This leads to a solid waste with a pH between 11 and 13. During stockpiling, the formation of carbonates like $Na_2CO_3$ or aragonite occurs [30]. The so-called “dry-stacking” of BR with <30 wt% moisture has become state or the art [17]. Currently, only small amounts of Bayer BR are used. Globally approximately 97% of the BR is landfilled [17]. BR valorization in China has increased substantially during the last three years, with an estimated utilization of 10–12%. This success is related to the use of BR as desulphurization reagent for the steel industry (K.A. Evans private communication, [56]) and will not be discussed in more depth. The national legislation, as well as toxicity classes of Bayer BR, differ. While most authors point out the environmentally concerning alkalinity and heavy metal contents of BR the literature does not assign toxicity classes (e.g. after EU regulation 1999/31/EG) to specific Bayer process residues and the BRs currently produced in Europe are classified as non-hazardous waste [24].

[1] Quartz-rich weathered bedrock containing iron and aluminate-rich hydroxyoxides [48].
[2] Eroded carbonate-based bedrock [48].
[3] Bauxites whose main Al bearing phase is diaspore (α-AlOOH). They show a lower solubility than gibbsitic ($Al(OH)_3$) and boehmitic (γ-AlOOH) bauxites) [50].

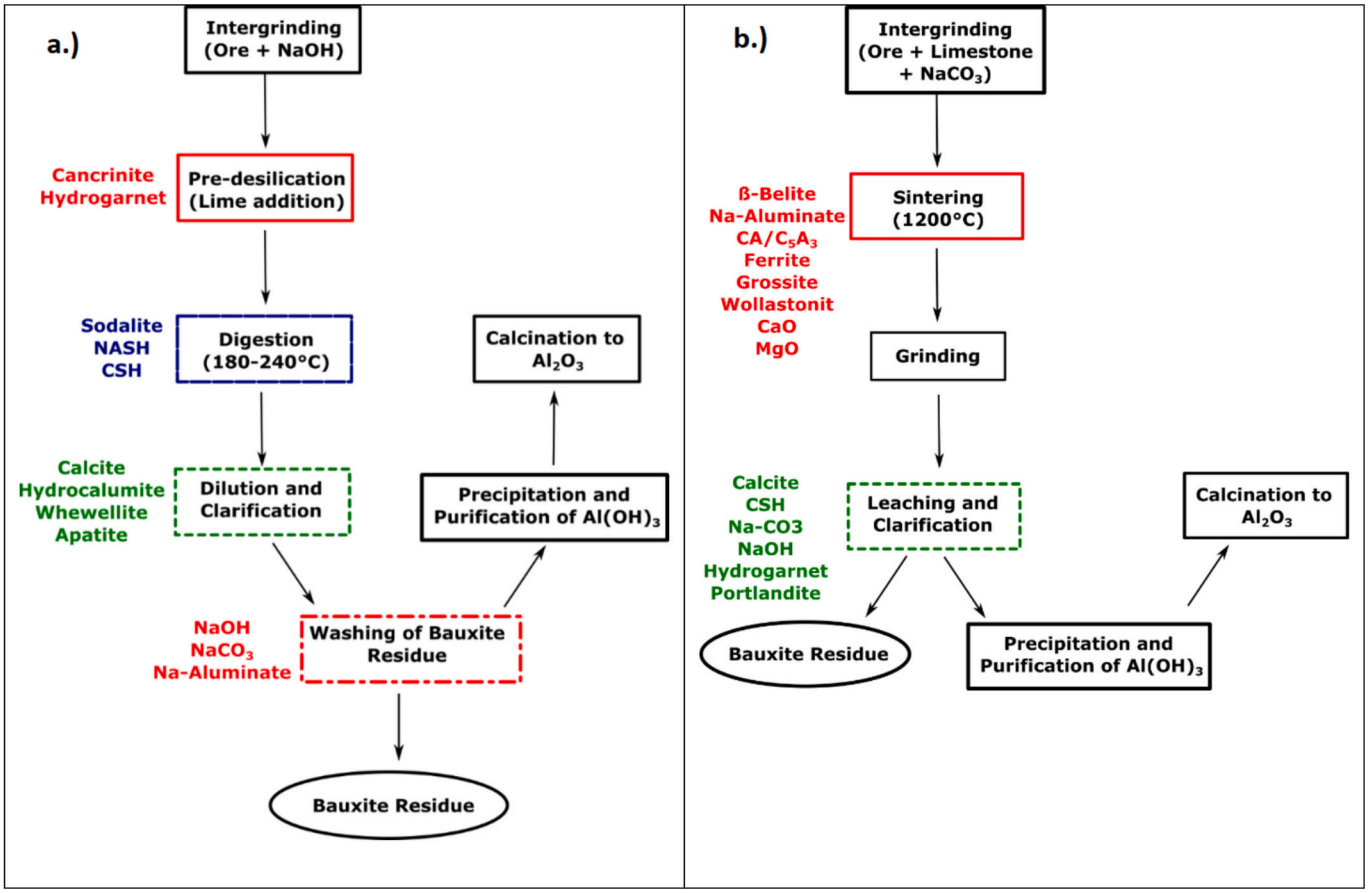


**Fig. 1.** Simplified flowchart of the a.) Bayer process [21,43] and b.) soda sintering process [36–39]. Phase names next to each step correspond to the main solid phases formed during this stage of the process that will form the Bauxite residue. This is highlighted by the colour choice that assigns the phases with the boxes symbolizing the different process steps.

### 2.2. The soda sintering process

The soda-sintering process is used for processing silicon-rich bauxites, nepheline, or aluminium-rich ashes [14,44,45,49].

$Na_2CO_3$ and limestone are interground with the raw material (Fig. 1b). During the sintering, belite, calcium aluminates, and sodium aluminates form. The sintered material is ground and leached in water, which leads to the formation of an alkaline solution and hydration products (e.g. hydrogarnet, portlandite, C-A-S-H) based on the soluble calcium-/sodium-aluminate phases. The resulting Al-rich green liquor is separated from the BR.

The soda sintering process is currently limited to plants in China, Russia, and Iran. Due to the incomplete dissolution of the sinter-phases, the BR contains significant amounts of β-belite [45,49,52]. This makes these BRs interesting for the cement industry. While the soda sintering process is less energy-efficient than the Bayer process, the development of hybrid processes may become relevant in the future [44].

Sintering process BRs are valorized as SCM or raw material for composite cement (e.g. coal-gangue/BR cements). These systems have been applied since the 1950s. Due to the limited volumes, the soda sintering process residues are of minor importance in the research targeting a valorization of BR in construction materials [49,57].

## 3. Characterization of BRs

To evaluate the potential of BRs in binders, their chemical and mineralogical composition needs to be analysed.

### 3.1. Elemental composition of bauxite residues

Fig. 2 shows the composition of BRs in the ternary diagram [Ca + Mg, Si, Al + Fe]. These elements are the main reactants in PC based cementitious systems [58]. A more detailed comparison between the element compositions of the shown materials is included in the supplementary information.

As references, other secondary cementitious materials (SCMs) and clinker systems (OPC and CSA) have been included. The SCMs can be separated into pozzolans (high silicon, low calcium) and latent hydraulic (low silicon, high calcium) materials. If a material has elemental compositions close to clinker, or common SCMs like fly ash, blast furnace slag, or silica fume, it can be expected to be well suited for composite cements or clinker production. While sintered BRs and hybrid (Sinter + Bayer) BR compositions are quite close to CSA clinkers and latent hydraulic SCMs, this is not the case for Bayer BRs. They contain less Si and Ca than pozzolanic or latent hydraulic materials, which makes their potential reactivity dependent on the soluble Al, Si, and Na content.

Table 2 gives an impression of the variability of element compositions published for Bayer and Sinter residues. It is restricted to the main elements in the oxidic form. More extensive data is provided in the supplementary materials (Table 4). Modern alumina plants try to maintain a relatively constant raw material feed, which is realized by mixing bauxite from multiple sources (e.g. karstic bauxite with lateral bauxites) to gain the largest amount of alumina from the lowest quality ores. The averaged composition given in the supplementary materials (Supplementary Table 4) shows a lower scatter than older data presented by Evans (2016) or Gräfe (2011) [17,30]. In each reuse scenario,

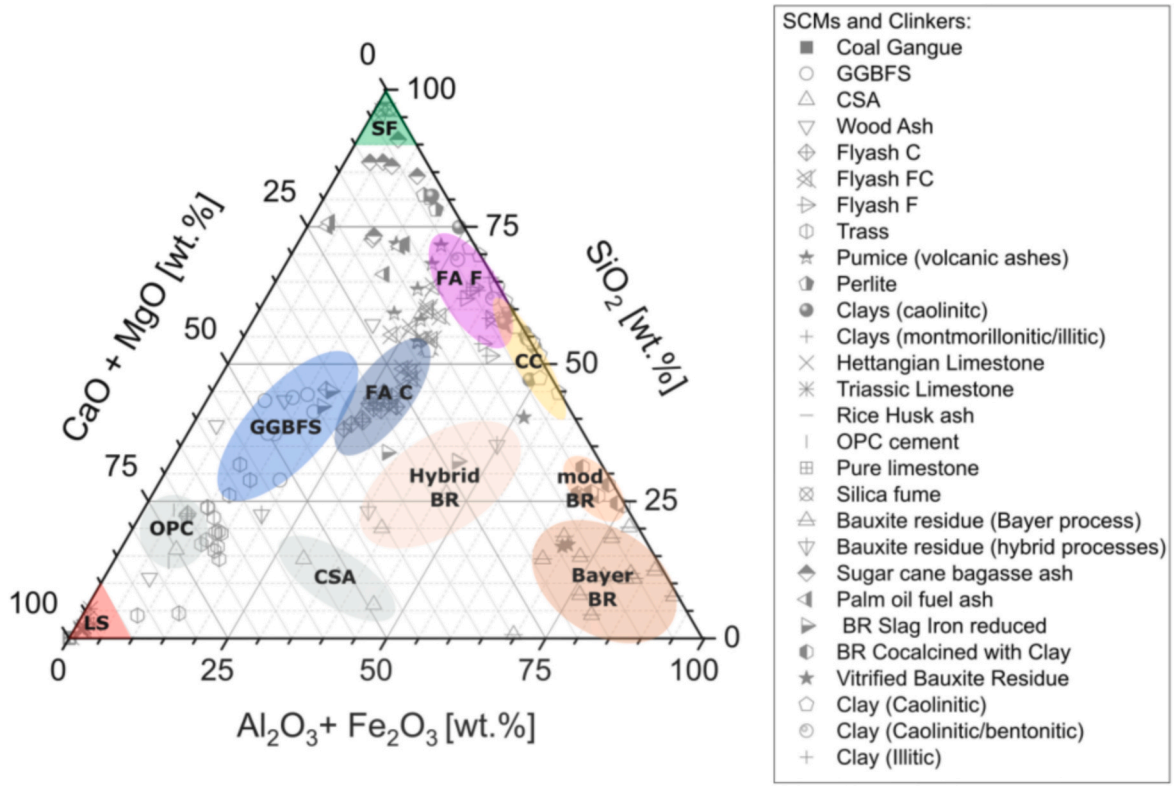


**Fig. 2.** Reactive oxide contents of BRs and other SCMs based on [8–14,28,29,51–87].

**Table 2**
Averaged oxidic compositions of BRs. The values are based on literature datasets, which are summarized in the supplementary materials [15–18,22,26,28,64,88–96].

| Oxide | Average oxidic composition [% wt.] |
|---|---|
| Bauxite residues Bayer process | |
| CaO | 6 ± 3 |
| $SiO_2$ | 9 ± 4 |
| $Al_2O_3$ | 18 ± 3 |
| $Fe_2O_3$ | 41 ± 10 |
| $Na_2O$ $_{(eqiv.)}$ | 5 ± 2 |
| $TiO_2$ | 6 ± 5 |
| LoI (loss on ignition) | 12 ± 7 |
| | |
| Bauxite residues sintering process | |
| CaO | 30 ± 11 |
| $SiO_2$ | 15 ± 2 |
| $Al_2O_3$ | 11 ± 4 |
| $Fe_2O_3$ | 16 ± 9 |
| $Na_2O_{(eq)}$ | 4 ± 1 |
| $TiO_2$ | 5 ± 3 |
| LoI | 15 ± 8 |

the BR's oxidic composition needs to be known. Cusack et al. could prove that its composition, even in one plant, varies over the years [104]. This is related to changes in the Bayer process, as well as variations in the digested bauxites. The most drastic change was induced by the introduction of dry stacking, which significantly reduces the amount of Na and Si in BR. This causes higher iron contents and a lower inherent reactivity of BR for the discussed reuse scenario [72]. The reactive contribution of Bayer BRs is mainly generated by the residual aluminate (15 ± 5 wt%), sodium hydroxide (5 + 10 wt%), and silicate (10 ± 5 wt %) present in the amorphous content and crystalline DSP phases (e.g. shown by [18]). Ca is present in DSP phases (mainly hydrogarnet and cancrinites) or carbonate minerals. The desilication process in particular is nicely reviewed in [105].

The reactive calcium is added in the desilication step to increase silicate precipitation, prevent the release of Ti (precipitation of $CaTiO_4$), and increase NaOH recovery. Therefore, BRs contain significant amounts of Ti (5 ± 5 wt%) and Fe oxides (40 ± 10 wt%). The iron-rich phases such as hematite, goethite or magnetite can be assumed to be largely inert, which is a common feature of iron-rich SCMs [36,106]. To our best knowledge, there is no publication focussing on the impact of iron on the hydrate phases in BR blended cements. Soluble Fe could participate in the formation of iron-rich Si-hydrogarnet [107], which has not been reported in the context of BR containing blended cements, but is predicted by thermodynamic modeling, and observed in other Al—Si-rich systems [107]. In case of very BR-rich systems, iron might even be included in phyllosilicate-like structures as reported in [108]. More research on the reactivity and phase assemblage of these systems is needed. The high loss on ignition values (10 ± 10 wt%) are related to residual water and organic residues originating from the bauxite ore (esp. humic acids and oxalates), flocculants and other process additives [55].

The element composition of BRs can be similar to other metallurgical wastes like copper-slags, water treatment sludges, and iron-rich clays [29,106]. The average amorphous content of Bayer BR ranges between 20 and 30 wt%, which is very low in comparison to e.g. slags or ashes (usually >60 wt% amorphous) [17,30]. This suggests that differences in the crystalline phase assemblage are important factors for BRs reactivity.

As indicated in Fig. 3 numerous trace elements, especially d-block metals and metalloids, are present in BR [40,98,109]. A good review of their distribution in BR is given by Vind et al. [110,111].

This review will not focus on the effects of trace elements on hydration, or their impact on environmental compatibility. The reason is the lack of data for BR containing cements. It is known that d-block metals, e.g. $Zn^{2+}$, can influence hydration kinetics [117], but no negative influences have been reported in BR blended cements.

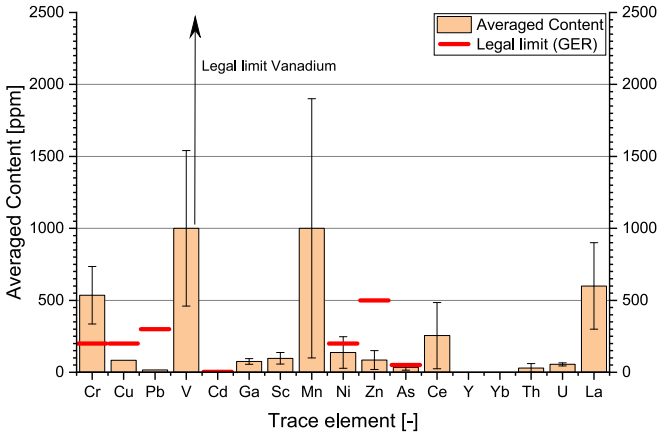


**Fig. 3.** Contents of minor elements in comparison to legislative limits according to LAGA 20 [112]. The error bars represent the scatter between the datasets of different publications [102,103–108,113].

It should be noted that Cr and Mn contents are critical factors in several country regulations e.g. they are higher than the German legislative limit for inorganic additives in concrete according to LAGA 20. These elements are usually the most critical ones, as illustrated in Fig. 3. Due to variations in the criteria for environmental compatibility between countries, no generic statement can be given. BR is a hydrometallurgical waste that is enriched in heavy metals and naturally occurring radioactive nuclides (NORMs). As reviewed in [40] the NORM contents of most BRs are uncritical for an application in the construction sector. Due to the dilution effect, the addition of up to 30 wt% BR to a cement would be possible without getting close to the current (2023) European threshold values.

### 3.2. BR mineralogy

The mineralogy of Bayer BRs is fundamentally different from sinter residues, which leads to a separate discussion.

#### 3.2.1. Bayer residue

Publications including quantitative phase assemblages of BRs are comparably rare but form a coherent image. As described in Fig. 1, the mineral phases of BR originate from four sources:

- Residual phases of the parent ore
- Precipitated as DSP during the digestion process
- Precipitated/added during dilution and clarification at lower temperatures
- Formed by hydration/carbonation during the storage of the BR

Table 3 presents an overview of the phases commonly found in BR. They can be classified as Fe-hydroxides, titanium oxides/perovskites, aluminium hydroxides, sodium aluminosilicates, and clay minerals.

The iron(hydroxy)oxides (hematite, magnetite, and goethite) are insoluble remnants of the parent ore.

The titanates and titanium oxides can be modified by aluminium extraction as shown by Vind et al. [110,111,118]. Rutile is not affected by the Bayer process, but an irreversible transformation of anatase to rutile occurs due to the high processing temperatures [119]. In the presence of $Ca^{2+}$ ions (e.g. due to a pre-desilication step), perovskite is precipitated, while already present perovskite remains inert [120]. Ilmenite (iron-titanium compound) is another inert minor of BR [121].

The aluminium(hydro)oxides are remnants of the leached main phases of the bauxite. Usually, boehmite is found, while sometimes diaspore, bayerite, and gibbsite are also present. Boehmite is a common minor phase in gibbsitic bauxites. These are preferred due to their low

**Table 3**
Mineral phases commonly found in Bayer BRs (e.g. [17,41,98,102,110,114–116]). The bold entries are very commonly reported in literature, while normal written minerals are often mentioned as minor phases. The italic font represents minerals only addressed in a few publications.

| Possible ICSD/ICCD codes | Minerals | Stoichiometric formula | Content range in dried BR [wt %] |
|---|---|---|---|
| Iron(hydro)oxides | | | |
| **71810** | **Goethite (Al substituted)** | **$Fe_{1-x}Al_xO(OH)$ X < 0.35** | **1 to 35** |
| **201096** | **Hematite** | **$Fe_2O_3$** | **10 to 30** |
| *30860* | *Magnetite* | *$Fe_3O_4$* | *0 to 8* |
| Titanium oxides/titanates | | | |
| *15409* | *Brookite* | *$TIO_2$* | *0 to 5* |
| **9852/ 93097** | **Anatase/ rutile** | **$TiO_2$** | **2 to 15** |
| e.g. 16688 | Perovskite | $CaTiO_4$ | 0 to 12 |
| 9805 | Ilmenite | $FeTiO_4$ | 0 to 5 |
| – | *Sodium titanate* | *$Na_2TiO_4$* | *0 to 5* |
| Aluminium(hydro)oxides | | | |
| **27865** | **Boehmite** | **AlO(OH)** | **0 to 30** |
| 04-009-3645 | Diaspore | AlO(OH) | 0 to 12 |
| 6162 | Gibbsite | $Al(OH)_3$ | 0 to 15 |
| *200413* | *Bayerite* | *Al(OH)3* | *0 to 5* |
| Sodium-aluminosilicates (DSP) | | | |
| **04-009-1974** | **Sodalite (part. X-ray amorphous)** | **$Na_4Al_3Si_3O_{12}OH$** | **4 to 40** |
| **04-024-2720/ 201367 ($CO_3$) 411048 ($NO_3$)** | **Cancrinite (two main species)** | **$Na_6Ca_2Al_6Si_6O_{24}(CO_3)_2$/ $NO_3(Na_{7.92}Al_6Si_6O_{31.56}N_{1.74})$** | **0 to 20 (50)** |
| *183563* | *Cancrisilite-$CO_3$* | *$Na_{7.4}$ ($Si_{7.44}Al_{4.56}O_{24}$) $(CO_3)_{1.41}$ $(H_2O)_2$* | *0–5* |
| Clay minerals and other hydroxides | | | |
| 74608 | Muscovite/ illite | $KAl_2(Si_3Al)O_{10}(OH)$/ $(K_{0.75}H_3O_{0.25})Al_2(Si_3Al)$ $O_{10}((H_2O)_{0.75}(OH)_{0.25})_2$ | 0 to 15 |
| 87771 | Kaolinite | $Al_2Si_2O_5(OH)_4$ | 0 to 5 |
| **172077** | **Katoite to Si-hydrogarnet** | **$Ca_3Al_2Si_3(OH)_{12}$** | **0 to 15 (partially X-ray amorphous)** |
| *202220* | *Portlandite* | *$Ca(OH)_2$* | *0 to 5* |
| Other silicates | | | |
| *89032* | *Schaeferite* | *$(Na_{0.7}Ca_{2.3})(Mg_{1.85}Mn_{0.15})$ $(Vo_4)_{2.88}(PO_4)_{0.12}$)* | *0 to 2* |
| *33685* | *Nosean* | *$Na_8Al_6Si_6O_{24}(SO_4)$* | *0 to 3* |
| *80835* | *Lawsonite* | *$CaAl_2Si_2O_7(OH)_2{}^*H_2O$* | *0 to 2* |
| *2937* | *Nepheline* | *$Na_3K(Al_4Si_4O_{16})$* | *0 to 2* |
| *9582* | *Zircon* | *$ZrSiO_4$* | *0 to 2* |
| **174** | **Quartz** | **$SiO_2$** | **0 to 5** |
| Other minerals | | | |
| 66333 | Dolomite | $CaMg(CO_3)_2$ | 0 to 5 |
| **73446** | **Calcite** | **$CaCO_3$** | **0 to 20** |
| *67435* | *Dawsonite* | *$NaAl(OH)_2(CO_3)$* | *Only legacy BRs in low amounts* |
| – | *Pyrite* | *$FeS_2$* | *0 to 1* |
| – | ***Amorphous*** | – | ***10 to 30 (Cu/ Co tubes) 0 to 10 (synchrotron radiation)*** |

**Table 4**
Composition of sinter BRs. The phases suggested for an XRD fit may need to be strongly modified or replaced. The contents were chosen to cover most of the data given in literature [44,45,49,52]. The highlighted minerals are either very common (bold) or rarely (italic) present.

| Possible ICSD/ ICCD codes | Minerals | Stoichiometric formula | Sintering process [wt%] |
|---|---|---|---|
| Clinker phases and oxides | | | |
| 81095 | γ-Belite | **$2CaO*SiO_2$** | – |
| 81096 | **β-Belite** | **$2CaO*SiO_2$** | **50–56** |
| 201096 | Hematite | $Fe_2O_3$ | Below 10 |
| 174 | Quartz | $SiO_2$ | Cross-contamination |
| 1880 | *$C_3A$* | *$Ca_{8.5}Na_1Al_6O_{18}$* | *Usually reacted* |
| 260 | *CA* | *$CaAl_2O_4$* | *Usually reacted* |
| 16191 | *Grossite* | *$CaO*SiO_2$* | *Usually reacted* |
| 98839 | **Ferrite** | **$4CaO·Al_2O_3·Fe_2O_3$** | **3 to 5** |
| 73446 | **Calcite** | **$CaCO_3$** | **2 to 12** |
| 66333 | Dolomite | $CaMg(CO_3)_2$ | Below 5 |
| Precipitated phases | | | |
| 94568 | **Perovskite** | **$CaO·TiO_2$** | **2 to 5** |
| | Sodium titanate | $Na_2TiO_3$ | – |
| – | Sodium silicate | $Na_2SiO_4$ | – |
| – | **NASH phases** | $Na_2O*xSiO_2*yH_2O$ | **Usually amorphous** |
| 202220 | Portlandite | $Ca(OH)_2$ | – |
| – | C-A-S-H phases | $CaO*xSiO_2*yAl_2O_3*zH_2O$ | Usually amorphous |
| 12645 | **Sodium aluminosilicate** | **$Na_2O·Al_2O_3·1.7SiO_2·2H_2O$** | **5 to 9** |
| – | Sodium aluminate | $NaAl(OH)_4$ | Often amorphous |
| 172077 | Katoite/Si-hydrogarnet | $Ca_3Al_x(SiO_4)_y(OH)_{3y}$ | Partially amorphous |
| | *Sodalite* | **$Na_{6+x}Al3Si3O12OHx*nH_2O$** | – |
| 201367 | *Cancrinite $CO_3$* | **$Na_6Ca_2Al_6Si_6O_{24}(CO_3)_2$** | – |
| 04-009-3645 | Diaspore | AlOOH | Below 5 |
| – | **Anorthite** | **$3CaO*Al_2O_3*0.6SiO_2*4.9H_2O$** | **5 to 9** |
| 71810 | **Limonites (example geothite)** | **$FeO(OH)*nH_2O$** | **4 to 10** |

digestion temperature. Their reduced availability led to the increasing use of boehmitic and even diasporic bauxites, as well as local bauxite resources of lower qualities. Furthermore, the formation of gibbsite (70–80 °C) and bayerite (RT) can occur during the dilution and clarification stage [122].

A main challenge in the Bayer process is the removal of silicon from the green liquor. The presence of silicates in the green liquor is caused by the partial dissolution of clay minerals and other reactive $SiO_2$ sources in the parent ore. The Si removal is needed to precipitate pure $Al(OH)_3$. Therefore, the desilication products (DSPs) are among the main phases of the BR. The DSP formation starts with the precipitation of amorphous sodium aluminosilicates, which transform into zeolite LTA (also called zeolite 4A), and then hydroxysodalite [125,126]. In case of high temperatures (e.g. digestion of karstic/diasporic bauxites at 230–250 °C) and the presence of $Ca^{2+}$ the hydroxysodalite transforms into cancrinite [127–129]. In parallel, the formation of siliceous hydrogarnet (HG) also takes place. At 245 °C 97.8% of the DSP is HG [130].

Typically, 40 to 60% of hydroxysodalite transform into a mix of different cancrinite stoichiometries in the BR. The transformation of sodalite to cancrinite is catalysed by the presence of $Ca^{2+}$ ions, hence by phases like calcite, hydrocalumite, or lime [128], and elevated temperature (e.g. 230–250 °C). $Ca^{2+}$ has a similar ionic size to $Na^+$ and partially occupies its positions in the cancrinite. Due to the higher charge density, it more effectively neutralizes the negative charge of the aluminosilicate cage, which may lead to a more stable structure and a better immobilization of silicate in the mineral. Xue et al. [128] could model the phase transition with a form of the Avrami equation and estimated an activation energy of 218 kJ/mol. Their findings suggest a nucleation and growth-controlled reaction. Due to the natural raw materials, foreign ions are present in these zeolitic minerals. In particular, the presence of carbonate and nitrate anions or chloride has been reported. Nitrates in Bayer liquor are mainly related to the decomposition of organic molecules originating from the raw materials or the flocculants added during the clarification process [125,128]. An increase in $CO_3^{2-}$ concentration limits HG precipitation and promotes cancrinite formation in a less crystalline DSP [130]. Especially in Bayer processes including lime addition, the reaction pathways are still not completely known. The addition of $CO_2$ in the Bayer process to generate less hydrogarnet and more reactive DSP phases should be investigated in more detail [130]. This is important, since the sodalite to cancrinite transformation is strongly impacted by the presence of the numerous ions present in the Bayer liquor, which leads to some researchers emphasizing that OH-sodalites and OH-cancrinite may not be the main crystalline DSP phases but less ordered "interphases" need to be assumed [125,130,131]. There are three main reasons for this; 1) the imperfect adherence of alumosilicate sodalites to loewensteins-rule leading to increased negative charges of the zeolite cages [132,133], 2) the presence of other cations e.g. $Ca^{2+}$ instead of $Na^+$ for charge balancing [127] and 3) the presence of alternative anions like $SO_4^{2-}$ or $NO_3^-$ instead of $OH^-$. These cause a distortion of the Al—O—Si angles and hence differences in the cage size. Detailed studies of the distortions occurring in impure OH sodalite frameworks due to the presence of foreign anions are given by [131,134–136].

Clay minerals are common impurities that partially dissolve during digestion. Only 2:1 phyllosilicates (muscovite/illite) are commonly detected in BR, but kaolinite can also be present. Quartz and zircon are Si-rich phases, that remain inert during the Bayer process. The same is true for most phosphate, sulfate, or carbonate-based minerals.

Simultaneously the formation of hydrates occurs during the hydrothermal process. Especially in the case of silicon-rich BRs, sodium aluminosilicate hydrates (N-A-S-H) precipitate. In principle, the formation of C-A-S-H also occurs if enough $Ca^{2+}$ is in solution. These minor phases are x-ray amorphous, which explains the missing quantitative information in the literature. In the Bayer process, the hydrate formation occurs before the precipitation of sodalite or cancrinite, if the residence time in the digestion reactor is long enough [43]. In the case of lime addition or Ca-rich bauxites, Lyu et al. report the formation of sodium hydroxide and tri-calcium aluminate instead of sodium aluminate. This phase is not stable and usually reacts with the excess of sodium silicate to form calcium aluminosilicate hydrates (C-A-S-H), HG, and portlandite as long as enough aqueous medium is present to enable dissolution and precipitation processes during (and after) the clarification step.

Besides "insoluble" alkalis, X-ray amorphous sodium aluminate precipitates. This can be partially removed by subsequent washing steps. While the formation of sulfate, or phosphate-containing sodium aluminates like nepheline, schaeferite, or nosean occurs, they can only be detected via synchrotron XRD [123].

Long-term BR storage leads to partial carbonation, causing the formation of carbonate containing sodalites/cancrinites, cancrisilites (another cancrinite-like zeolite), and carbonates like calcite, dawsonite (carbonation of residual sodium aluminate) and $Na2O_3$ (natrite) (carbonation of excess Na(OH)) [137].

It should be noted that a large variety of organic compounds is present in BR [20,30,43]. Guo et al. reported total organic carbon (TOC) contents of 4 ± 1 g/kg [138]. Currently, not enough data are published to give an average. The presence of organics is related to the organic compounds of the bauxite and flocculants (their decomposition products) used during phase separation. The most common compounds are sodium salts of polyhydroxy acids, humic and fulvic acids, as well as sodium succinate, acetate, and oxalate. Additionally, phenols and alcohols may be present [139]. They are usually X-ray amorphous. The

presence of whewhellite ($Ca(C_2O_4)\cdot H_2O$) has also been reported [43].

X-ray diffraction is the most suitable method for quantifying crystalline phases and visualizing trends in BR mineralogy. The main sources of errors are the overlapping of peaks and the choice of phases during analysis (operator bias). Especially the substitution of aluminium in iron minerals and the presence of numerous minor elements [118] is almost impossible to consider properly and often leads to an overestimation of the Fe content in the bulk sample [140].

Feret et al. identified many of the minor phases of BR in their quantitative synchrotron-XRD investigations on multiple BRs [123]. Synchrotron radiation drastically reduces peak broadness and allows the quantification of more phases (e.g. to distinguish between $NO_3$ and $CO_3$ cancrinites) in comparison to lab XRD equipment. The method also allows quantifying phases with more distorted lattices (e.g. precursor phases of sodalite) and small crystallite sizes e.g. hydrogarnets. These phases contribute significantly to the amorphous content in laboratory XRDs, as researchers showed by comparing results of element analytics with Rietveld results [36,123,124]. The amorphous content of synchrotron measurements (0 to 10 wt% [124]) is significantly lower than the one measured with laboratory diffractometers (20–30 wt%).

#### 3.2.2. Sintering process BR

The literature about quantitative phase assemblages of BRs from the sintering process is scarce (see Table 3). More data would be needed to enable a better quantification of these materials. The most important minerals reported by Liu et al. [43] are clinker phases like belite and ferrite, which remain partially unreacted after leaching the sintered material during the process. Phases like CA and $C_3A$ have only been reported qualitatively. Usually, also feldspars (anorthite) and iron hydroxides like goethite are present in significant amounts. Calcium aluminates should only be present in low amounts, due to their dissolution during the leaching step. In this step perovskite, sodium silicate, N-A-S-H/C-A-S-H phases (X-ray amorphous), and portlandite precipitate. No quantitative data could be found.

### 3.3. Physical properties of Bayer BRs

Determining the correct particle size distribution of BRs is difficult, due to sampling issues and the strong agglomeration of the primary particles. Most BRs have mono or bimodal PSDs with $d_{10} \approx 0.7 \pm 0.3$ µm, $d_{50} \approx 10 \pm 5$ µm, and $d_{90} \approx 40 \pm 30$ µm (see Supplementary Table 7). BRs do not need to be ground to reach cement fineness. However, single particles with diameters of several mm are reported [141]. The reported specific surface areas of BRs are $20 \pm 10$ $m^2/g$ ($N_2$ BET adsorption) [18,30,35,38,97,98,102,142,143]. Bulk densities of materials like BR are best determined via He-pycnometry. Older literature (e.g. [144]) reports surprisingly low densities between 0.7 and 2.2 $g/cm^3$. This is the case because at this time BR slurries were common. Today, BR is filter-pressed and has an average bulk density of $3.7 \pm 0.3$ $g/cm^3$ (raw data supplementary materials Table 5) [72,145]. The density of BR mainly depends on the content of Fe-rich minerals and the residual moisture content as illustrated by Gräfe et al. [30]. Different from most SCMs, filter pressed and dried BR (both processes are necessary if BR is to be utilized in cementitious systems) has a higher density than OPC (approx. $3.1 \pm 0.1$ $g/cm^3$). Thermochemical activation processes lead to a density reduction e.g. from 3.43 to 3.27 $g/cm^3$ in the case of co-calcination with clay (own results).

## 4. BR reactivity in OPC systems and BR activation

The use of BR, especially its dealkalized coarse fractions [109,146–148], as alternative aggregates has been investigated [149].

However, most BR valorization approaches focus on cementitious binders and SCMs. Therefore, the use of BR as artificial aggregate will not be further discussed in this review.

Currently the main construction material related application of BR on an industrial scale is the use as iron-corrective for clinker burning. This mainly occurs on a national scale, since the shipping of BR does not only require filter-pressing (problem of liquefaction during transport) but also entails regulatory issues [24].

Elakneswaran and others showed that the production of iron-rich OPC clinkers is possible without changing the hydration pathways [150]. The main difference to common OPC is an increase in ferrite (15–18 wt%) and a reduction in belite (<10 wt%). The main benefit of these clinkers is their lower firing temperature (1350–1400 °C) [142–144]. Their strength development was described to be comparable to standard cements as found in EN 197-1. Adding >3 wt% BR is not recommended due to the extra sodium input causing problems with process stability [17,49,153,154]. Furthermore, increasing amounts of Fe-rich melt reduce the life-time of rotary kiln refractories which explains why cement companies are not pursuing this approach. A significant number of publications target BR utilization in geopolymer binders and CSA cement. The potential of BR as precursor for geopolymerization has been reviewed by Hertel and Pontikes [155]. For CSA-type cements, multiple case studies prove that BR is suitable for burning, largely waste-based, CSA clinkers [26,92,100,136–140]. The hydration, and the influences of minor phases (caused by impure raw materials like BR) of CSA systems has been reviewed by Ben Haha et al. [161], but a review specifically targeting the characteristics of BR containing, waste based CSA clinkers is missing.

**Table 5**
Reactive phases in untreated and activated BR residues. The thermally induced transformations of the BR phases have been assumed based on simplified systems analysed in literature [87,151–160]. Bold phases are usually present, while italic phases are rarely present. The abbreviations mean pozz. = pozzolanic, lat. hy. = latent hydraulic and hy. = hydraulic reactivity. Stoichiometric formulas are provided in Table 2 and Table 4.

| Reactive minerals and phases | Thermochemical treatments | Hydration products | Reactivity |
|---|---|---|---|
| **Sodalite** | Untreated BR | AFm*, AFt, C-A-S-H | Pozz. |
| **Cancrinite** | | AFm, AFt, C-A-S-H | Pozz. |
| Sodium aluminate | | AFm, AFt, C-A-S-H | Pozz. |
| *Cancrisilite-$CO_3$* | | AFm, AFt, C-A-S-H | Pozz. |
| *Nosean* | | AFm, AFt, C-A-S-H | Pozz. |
| *Portlandite* | | C-A-S-H, AFm, AFt, CH | Lat. hy. |
| Kaolinite | | AFm, AFt, C-A-S-H | Pozz. |
| **Sodalite (dehydroxylated)** | BR co-calcined with clay 700–800 °C | AFm, AFt, C-A-S-H | Pozz. |
| **Cancrinite (dehydroxylated)** | | AFm, AFt, C-A-S-H | Pozz. |
| *Cancrisilite-$CO_3$* | | AFm, AFt, C-A-S-H | Pozz. |
| *Mayenite/***amorphous aluminosilicates** | | AFt, AFm, C-A-S-H | Pozz. |
| Nosean | | AFm, AFt, C-A-S-H | Pozz. |
| *Free lime* | | C-A-S-H, AFm, AFt, CH | Hy. |
| Amorphous aluminosilicate gel | | AFm, AFt, C-A-S-H | Pozz. |
| **Metakaolin and other metaclays** | | AFm, AFt, C-A-S-H | Pozz. |
| Part. amorphous silicate | | C-A-S-H | Pozz. |
| **Ca/Na aluminosilicate glass** | BR molten with additivation >1250 °C | AFm, AFt, C-A-S-H | Pozz./lat. hy. |
| *Akermanite* | | AFm, AFt, C-A-S-H | Pozz./lat. hy. |

* Depending on the availability of Ca and $SO_4$, as well as $CO_3$ different AFm phases may form, no specific publications on this topic are available.

Due to the potentially larger replacement volumes and the compatibility with commercial clinkers, the use of activated BR as SCM has more potential. Therefore, this review focuses on the application of BR as SCMs.

### 4.1. Reactivity of Bayer residue

The first reports of the pozzolanic activity of sodalite and cancrinite were published by Takeuchi [162,163]. Ribeiro et al. show a low pozzolanic activity of BR (Pozzolanicity Index = 0.79 surpasses the required 0.75 according to NBR 5752) [18]. New results using the so called $R^3$ test [93] also show that BR can be considered as reactive SCM [35].

Several authors confirm that the elevated sodium contents of BR lead to an acceleration of the hydration reactions. They do not clarify if the contribution of the DSP only relates to improved early age performance, which highlights the need for long-term hydration studies of such systems [18,38,164].

The comparatively low pozzolanic reactivity of BR is due to its high fraction (typically 70 to 90 wt%) of chemically inert phases (mostly iron (hydroxy)oxides). An overview of the reactive contributions of the main phases is given in the Supplementary Table 8). Table 5 summarizes the typical reactive phases found in BRs and BR-based SCMs and their hydration products if used in blended cements.

Untreated BRs are not reactive enough (see Section 6) to compete with common SCMs like fly ash. A replacement of 30–50 wt% causes significant performance losses (strength evolution, rheology etc.) and is only reported by Senff et al. [38,165]. This led to the conclusion that chemical or thermochemical treatments are needed if an industrial valorization of BR is targeted.

### 4.2. Thermodynamic modeling of sodalite under simplified cement conditions

Besides ensuring sufficient reactivity, it is important to know which hydration products are formed by the reactive phases in BR to lay the foundation for explaining the engineering and durability properties of the resulting concrete.

Danner et al. [35] showed that significant portlandite consumption occurs if BR is mixed with it. They assume the formation of AFm phases from DSP, which is supported by other publications [36,164]. The current data is not sufficient to say if BR has an impact on AFm stoichiometry. Manfroi et al. also report the formation of C-A-S-H in blended cement pastes [164]. The shift towards a higher inclusion rate of tetrahedral Al in the silicate dreierketten of C-S-H is catalysed by the elevated pH due to higher sodium contents. This mechanism has been illustrated on Na-spiked white cement by Skibsted and Andersen [174].

The same reaction products are expected for modified BRs since the DSP is combined with further aluminosilicates that enhance the pozzolanic reactivity [36,95].

Hydration reactions are based on dissolution and precipitation processes, which are often described through thermodynamic modeling [175,176]. The expected equilibrium state (the stable composition of the system ignoring kinetic effects) of the DSP in the presence of $Ca(OH)_2$ and $CaSO_4$ can be shown by calculating the thermodynamic equilibrium of a simplified system using the GEM-Selector software [177,178] with the PSI-Nagra, Cemdata (18.01, with CSHQ model) and zeolite21 (21.02) thermodynamic databases. For the calculation of the aqueous solution speciation, the extended Debye-Hückel theory (Helgeson [179]) was used with the parameter set for Na(OH), because Na(OH) is the strongest base present in the system. The detailed system input and process scripts are given in the supplementary material (Table 9).

Fig. 4 shows the pozzolanic reactivity of the DSP. It can be seen that the reaction of 1 g sodalite consumes roughly 1.3 g of portlandite. Depending on the supplied amount of calcium the hydration products change from C-A-S-H and straetlingite to C-A-S-H phases and katoite.

At very low Ca concentrations sodalite is dissolved and precipitates as zeolite A4, which is its poorly crystalline precursor in the DSP [128]. Sodalite precipitation has only been reported at temperatures of <100 °C and pressures of 1–120 bar. In simplified systems containing C-S-H, ettringite, and albite ($NaAlSi_3O_8$) at 20–50 °C the presence of zeolite X has been reported by Lothenbach et al. at [180]. Zeolite X

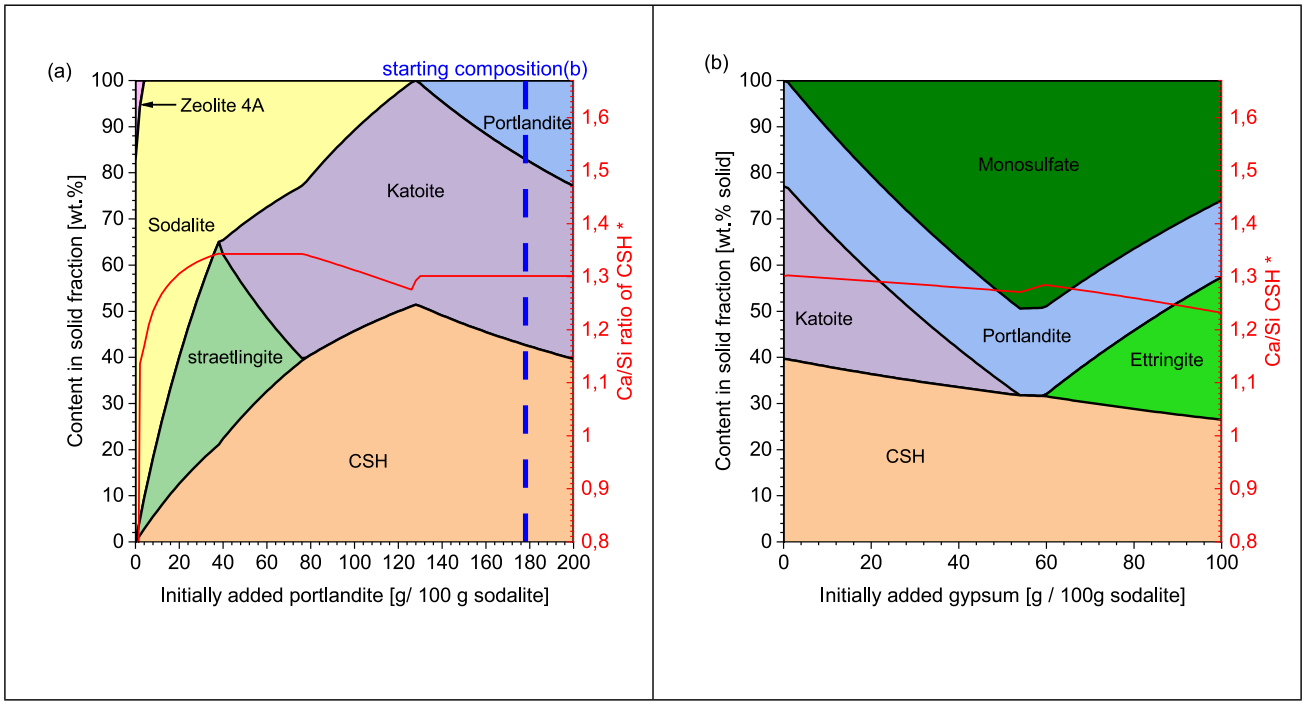


**Fig. 4.** Thermodynamic simulation of the reactions of (a) sodalite and portlandite; (b) sodalite and portlandite (100 and 175 g), and gypsum at w/s-ratio = 2. Only the composition of the solid fraction is depicted. *The depicted Ca/Si ratio is lower than expected (approx. 1.67) because significant amounts of the CSHQ models NaSiOH endmember are predicted.

contains more silicate and less Na than the similar zeolite A. The shift of the zeolitic forms may be caused by the higher alkali contents, pH values and Al/Si ratios in the simplified BR system. Straetlingite and katoite [82,181] are known to precipitate in sulfate and calcium-deficient blended cements with high contents of reactive aluminate and silicate. For Fig. 6(b) a SOD/CH ratio of 100/175 g/g was chosen, to simulate the conditions in a 20 wt% BR containing blended cement. This is the highest reasonable cement substitution with untreated BR. In this mix design sodalite contents between 2 and 6 g/100$g_{binder}$ are expected. This point is highlighted by the dashed line in Fig. 6(a). The solid fraction contains roughly 20 wt% CH similar to an OPC system [182]. Because no phase assemblages for BR blended cements have been published this value was chosen. In real systems lower CH values are to be expected. We decided against a lower CH excess in Fig. 6(b), because a consumption of an equivalent 15 wt% of CH similar to $LC^3$-50 systems [183] seems unreasonable. Since cements contain sulfate, the marked composition of Fig. 4a) is equilibrated with increasing amounts of sulfate. The results (Fig. 4(b)) show that katoite is replaced by monosulfate as soon as sulfate is available. This happens because the formation of al-siliceous hydrogarnet was blocked, according the guideline in [cemdata07]. However, in iron-containing systems, an Al—Fe siliceous hydrogarnet solid solution is expected [184].

At sufficiently high sulfate contents only C-A-S-H (Ca/Si = 1.3–1.2), $SO_4$-AFm, and AFt precipitate. It needs to be pointed out that the CSHQ model was used in this simulation. Besides endmembers defining the upper and lower threshold values for tobermorite and jennite like CSH this model also contains KSioH and NaSiOH endmembers that depict the structural transition to geopolymers. In our simulation significant amounts (up to 40% of the CSH) of the NaSiOH endmember were found, which explains the reduction of the average Ca/Si ratio from 1.6 to 1.3. To clarify if the chosen modeling strategy depicts reality further research is needed. This would match well with the reported mineralogical changes of BR-containing cements. A main limitation of this model is, that it does not include any kinetic impacts due to the dissolution of BR. Therefore, experiments with synthesized OH-Sodalite are recommended to detect kinetic effects and validate the simulations.

While Ma et al. provided important thermodynamic data for some zeolites [170–172], iron, heavy metal and anion impurities (esp. carbonate and nitrate) present in industrial residues are not yet taken into account. Pure phase synthesis alongside the determination of solubilities and dissolution enthalpies/formation enthalpies is still needed for some phases present in BRs, and (especially) modified BRs.

The impact of the mostly sodium-rich zeolites on the composition of formed AFm and C-A-S-H phases needs to be specified, since these phases are well known to include alkali ions in their interlayer or adsorb them on their surfaces [188–190], this process is reported to be more pronounced in pozzolanic C-A-S-H [191]. This implies an increase of Na immobilization in aluminate rich blended cements that contain aluminate rich C-A-S-H phases and elevated AFm contents. It should be investigated if high replacement levels lead to the presence of N-A-S-H-gel and/or Na substituted AFm phases such as the U-Phase [192,193].

### 4.3. Activated Bayer BR

Due to the BR's low initial reactivity several activation approaches have been tried. They can be grouped into thermochemical treatments and carbonation methods.

#### 4.3.1. Chemical activation of Bayer BR

One approach towards low-clinker BR blended cements is the development of ternary systems that combine the alkali activation of BR (5 to 10 wt%) with an additional pozzolanic or latent hydraulic contribution of a second SCM (20 to 60 wt%).

This synergistic effect is one of the reasons for not utilizing dealkalized BR in blended cements. If dealkalized BR is going to be used as SCM only carbonation and $Ca(OH)_2$ based dealkalization treatments can be applied to reduce the soluble Na levels. The reason for that is the introduction of foreign anions (mainly $Cl^-$, $SO_4^{2-}$ or organic) during acid-based approaches, which influence the hydration of the cementitious systems in a negative way. A comprehensive review of existing BR dealkalization technologies is given by [43]. In the case of $Ca(OH)_2$ based dealkalization the BRs pozzolanic DSP is dissolved during the process and forms C-A-S-H and Si-hydrogarnet, leading to a CH containing, otherwise inert, filler as indicated by [194]. Publications dealing with dealkalized BR as a binder component are scarce. Positive results of a Na-Acetate based BR dealkalization on the performance of a cementitious binder are only reported by Danner and Justnes [195].

If the focus of BR blended cements is set on non-structural applications the use of dealkalized BR is quite promising for utilizing large BR volumes e.g. in paving-stones or road base binders. The approach is convincing since only filter-pressing and solar drying are needed for preprocessing the BR.

Much more promising are ternary binders where BR is combined with a second SCM with low alkali content to dilute the system and immobilize some Na in the formed AFm and CASH phases. To the authors knowledge ternary systems containing untreated BR, silica fume, fly ash [193,196–198], steel slag [199] and GGBFS [200] have been investigated. Especially the combination of BR with latent hydraulic wastes proved efficient, because the slight alkali activation increases early age hydration of the SCM rich (up to 70 wt% BR and steel slag/GGBFS) blended systems, making them well suited for prefabricated parts [199,200]. Zhang et al. reported a strength evolution corresponding to a CEM 52.5 for a binder containing 30 wt% OPC,30 wt% steel slag, 30 wt% GGBFS and 8 wt% of BR [200].

The results imply that the BR addition activates clinker and pozzolanic SCMs according to the well-known effect of increased alkali contents on the hydration of OPC (blended) cements [201–203]. Only semiquantitative proof of this hypothesis is given by [204] for the BR/metakaolin/OPC system and by Hao et al. for the BR/steel slag/OPC system [199].

With calcined clay, or thermally activated natural pozzolans, the thermal treatment of the main SCM can either be carried out with or without BR, marking the border between chemical and thermochemical modification.

While this scenario is the best case for the alumina industry, the binder's sustainability is strongly dependent on the $CO_2$ footprint of the second SCM. Nevertheless, such ternary binders may be a main pathway towards BR valorization. Here more systematic research with a large variety of bio ashes, carbonated concrete fines, calcined clays and similar emerging SCMs, as well a direct comparison to established reference systems are needed. Especially data on durability performance and microstructural evolution of these ternary binders are lacking.

#### 4.3.2. Thermochemical activation of Bayer BR

The investigated thermochemical treatments are summarized in Fig. 5, while an impression of the impact on reactivity is visualized in Fig. 6.

The least energy consuming method to activate BR is calcination at 700–800 °C. Here inert aluminium (hydro)oxides and carbonates are decomposed.as well as the hydrate phases (HG,N-A-S-H/C-A-S-H) [101,144,166,167,205]. These processes lead to a higher availability of reactive aluminate and silicate [144].

Several publications confirm a calcination-induced increase in the reactivity of Bayer BR [206–208]. The optimum calcination temperature range is between 700 and 800 °C [39,168,169,209]. Ye et al. confirmed that these conditions led to a maximum Si and Al release at alkaline pHs, which implies a reactivity maximum in cementitious systems [209]. This temperature range is the optimum for silicate/aluminate bearing phases at reasonable process times.

To increase BR reactivity enough to enable BR contents of 30 wt% or more in blended cement, the increase of Al and Si availability is needed [29]. This leads to SCMs similar to those explored in the RemovAl

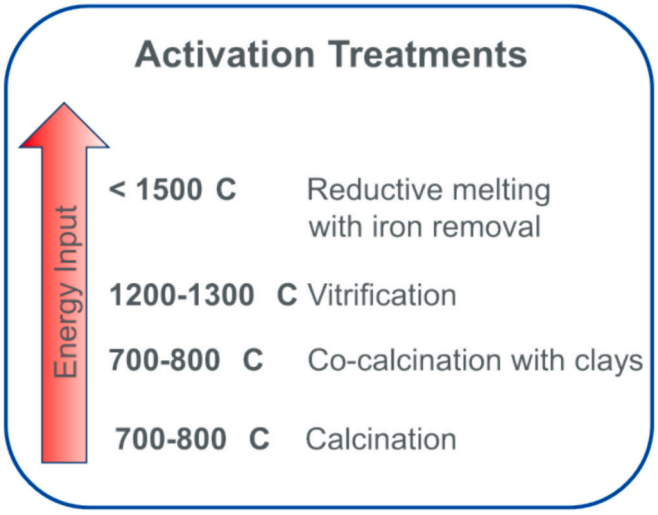


**Fig. 5.** The reviewed thermochemical activation methods for BR-based SCMs.

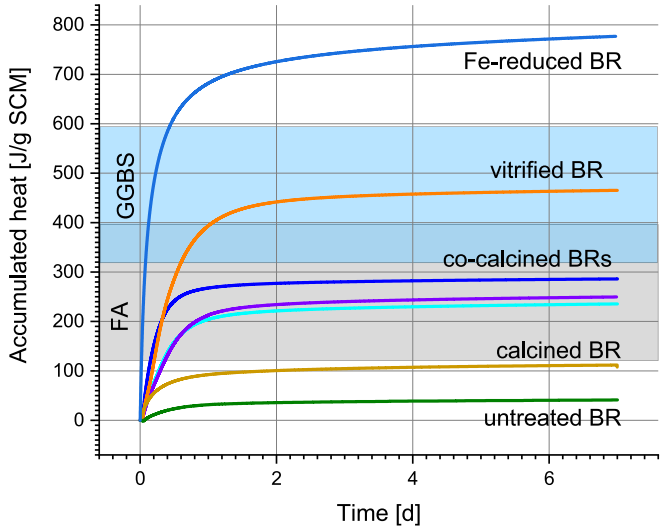


**Fig. 6.** Pozzolanic reactivities of European BR, in different stages of modification, determined by the $R^3$ test. The results were obtained by the application of standard C1897-20 (own research with details given in the supplementary materials and [36]).
The ranges for FA and GGBFS are taken from [221].

[210,211] and ReActiv [36] projects.

A low-energy approach is the co-calcination of BR with other, aluminosilicate rich, precursors. While first co-calcination experiments were carried out with fly ash [212], the use of clays is more promising [35,36]. The main reasons are material availability and environmental compatibility. The formation of metakaolin (400–700 °C) and/or reactive smectic metaclays (600–950 °C) aligns with the temperature range for BR calcination (700 to 800 °C [213]). This approach has been introduced by Danner et al. to reduce the soluble alkali content of BR [35]. It also increases BR reactivity [36]. It could be confirmed that reactivities comparable to fly ashes can be achieved by adding 10 to 20 wt% of kaolinite to BR [36]. The reactivity of co-calcined BR is dependent on the amount of initial DSP and added kaolinite [36]. Peys et al. could show a synergistic effect between metakaolin and BR [36]. The increased alkalinity of the blended cement should serve as a mild alkali activation leading to faster hydration kinetics of the blended cement. Heavy metals, like $Cr^{3+}$, are partially immobilized in metakaolin and its hydration products [36].

The most efficient way to activate all silicates and aluminates in BR is vitrification (1200–1300 °C). In this process the fluxed BRs mineralogy is completely transformed into reactive glass phases and inert phases. Fluxes like CaO, $B_2O_3$, $Na_2O$, or $SiO_2$ ensure a eutectic composition and low melting temperatures [37,95,173,210]. Changes in additivation ensure a constant, BR independent, reactivity of the glass phases. This results in a well performing SCM [210]. A reducing atmosphere is suggested by Giels et al. to prevent the formation of metallic iron and other detrimental components (e.g. $Cr_2O_6$ [173]).

Materials like recycled concrete fines, low-grade limestones, quarzitic rocks, or silicon-rich ashes can be used to adjust the chemistry of the vitrified BR. Giels et al. reported reactive slags based on up to 80 wt % BR [173]. Depending on additions, cooling rates, and treatment temperatures, large variations of amorphous content (20–80 wt%), as well as composition and amount of crystalline phases can be observed [37,95,157,214]. Spinel formation (magnetite ($Fe_3O_4$)–hercynite ($FeAl_2O_4$) solid solution) is to be expected and should have a beneficial effect on the immobilization of heavy metals like Cr or V. Parts of the DSP may transform to plagioclase (tectosilicate, (Ca, Na)$Al_2Si_2O_8$) or nepheline [95,173]. Bullerjahn and Bolte also reported the presence of akermanite-gehlenite and quartz [37].

A complete melting of BR using the Pedersen process (carbothermic, CaO, and $SiO_2$ fluxes [215], 1500–1600 °C) allows the recovery of titanium carbide and iron, while generating reactive slags (see Fig. 6). Ca is added to the system to serve as a fluxing agent and immobilize silicate and aluminate in very reactive, aluminate-rich Ca silicate glass and crystalline phases. Hertel et al. report the presence of spinels and >95 wt % of glass phases, which is not described in other publications [211]. The presence of β-$C_2S$, $C_3A$, mayenite and CA has been reported regularly [180,184–188]. Sodium aluminosilicates are not always present in detectable amounts, glauconite (very heterogeneous layered aluminosilicate with alkalis and trivalent metals), sodium aluminium silicate and anorthite (Ca($Al_2Si_2O_8$)) have been reported [216]. Residual carbon and perovskites could also be expected. Despite the differences in mineralogy, the element composition is similar ($Na_2O$ 2.2 ± 0.5, $Al_2O_3$ 36 ± 5, $SiO_2$ 10 ± 6, CaO 45 ± 8, $TiO_2$ 2 ± 2 wt%) [180,184–188,217,219]. The reactivity of these phases concerning hydration reactions has not been systematically investigated. Most research involving this type of thermal treatment targets the recovery of rare earth metals or residual aluminium and hence lacks a sufficient characterization of the formed slags before the subsequent leaching processes [215,217,219]. Bullerjahn and Mehringskötter showed that the production of GGBFS-like slags from BR is possible [220].

The discussed thermochemical activation technologies have only been researched in the lab scale, which makes a detailed LCA of these SCMs impossible. The Electrification of oven technology has a large potential to reduce the carbon footprint of these materials, because the lack of carbonates leads to almost no process intrinsic $CO_2$ emissions. Upscaled results need to be generated before a final evaluation of the technologies is feasible. Especially the reductive smelting or vitrification of BR may not be a sustainable reuse option. The Pedersen process route needs to rely on added value (both ecologically and economically) generated through the production of pig-iron or TiC/ferrotitanium alloys to be a viable route for BR valorization.

### 4.3.3. *Carbonation of BR*

The carbonation of BR has been researched as a dealkalization treatment [99] to use the BR as a soil remediation additive [43]. Wet or semi-dry carbonation is investigated as an approach to activate alkali/earth-alkali aluminosilicates and their hydrates. Wet carbonation at high $CO_2$ partial pressure and elevated temperature (60–70 °C) leads to a fast (30 min to 1 h) and complete carbonation of the targeted minerals (mainly HG) [222].

The enforced carbonation leads to the formation of carbonates and a reactive aluminosilicate gel [223–225], which indicate a possibility to use carbonated BR as SCM. In carbonated BR the presence of natrite

($Na_2CO_3$), dawsonite ($NaAlCO_3(OH)_2$, nacolithe ($NaHCO_3$) and trona ($Na_3(HCO_3)(CO_3)*2H_2O$) has been reported. Aluminate surplus causes the formation of Al-hydroxides (e.g. bayerite) [137,226]. Furthermore, hydrate phases like hydrogarnet or C-A-S-H decompose, while zeolitic sodium aluminosilicates remain stable [137,222].

Another knowledge gap is the influence of the alkali carbonates on pore solution pH and composition. Several authors [193–196] report reduced pH values for carbonated BRs. The $NaHCO_3/Na_2CO_3$ species buffer the solution at pH 10 to 11 instead of 11–13 for the untreated material. To evaluate the potential of this approach hydration studies with carbonated BR are needed.

### 4.4. Bauxite residue from the sintering process

The sintering residue is a latent hydraulic material. Its reactivity is mainly based on belite and residual calcium aluminates, while sodium aluminosilicates formed during the digestion give a pozzolanic contribution. Zhang et al. showed that sintered BR in combination with coal gangue is reactive enough to form a cementitious material [228].

The main hydration products are C-A-S-H, ettringite and portlandite [208,228]. Other experiments made with GGBS, gypsum, and other waste materials led to performant binders of CEM 32.5 quality [52,103]. The BRs reaction in binary systems with OPC should be sufficient and of a latent hydraulic nature. Isothermal calorimetry data quantifying the reactivity of sinter BR have not been published in English literature. The use of sintering BR for the production of commercial cement has been reported [49].

## 5. Bauxite residues in concrete

In the following sections we present data generated with equivalent methods and very similar mortar or concrete mix-designs, to point out correlations between the hydrated binder's microstructure and macroscopic properties. If a wider range of datasets is compared most differences in transport properties and even strength development may be related to the applied mix-design and not the influence of the added SCM. The taken approach allows to draw first conclusions for developing mix-designs tailored for BR containing blended cements, while also providing a benchmark with more common blended cements. Additional datapoints are given in the supplementary materials.

### 5.1. Early age and engineering properties

To meet the various Net-Zero concrete roadmaps [229,230] high substitution levels (30–50 wt%) have to be targeted. As discussed before untreated BR shows a much lower reactivity than common SCMs. This restricts high replacement levels to non-structural applications like tiles, pavement bricks, or road-based material [231]. Senff et al. showed that mortars with up to 40 wt% untreated BR (dosed as a slurry instead of filter-pressed material) can be made [38]. Most other sources restrict themselves to BR contents lower than 20 wt% [18,38,165,232]. The main reasons are an increased water or superplasticizer demand and insufficient strength development, as well as potential issues with environmental compatibility (see Sections 2 and 3).

#### 5.1.1. Workability and rheological studies

BR addition leads to a higher viscosity of pastes and mortars [233,234]. A decreased workability is common for SCMs with very high specific surface areas (e.g. calcined clays), and leads to an increased water and superplasticizer demand. However, BR-based SCMs that are produced via vitrification or smelting show rheological properties comparable to OPCs [37,235] or slag blended cements. The same is true for ternary binders, containing 5 to 10 wt% of BR and 30 to 60 wt% of slags or fly/bio ashes.

Comparing rheological data of cement pastes or mortars is difficult, due to varying rheometer geometries and measuring conditions. Only general trends can be compared. To give an impression of the impact of the BRs thermal treatment on the workability timeframe the static yield stress of 30 wt% SCM containing binders is depicted in Fig. 7a. The pastes were made without the use of superplasticizer at a w/b ratio of 0.5 to remove any differences besides the SCM type from the experiment. Details of the measurement protocol can be found in the supplementary materials. The samples show a non-linear increase in static yield strength, which is most pronounced by untreated and co-calcined BR. Only these SCMs contain zeolitic sodium aluminosilicates and higher (1–2 $m^2$ g OPC versus 12–20 $m^2$ g co-calcined BR) specific surface area, while vitrified BR and OPC reference do not. If this difference in structural build-up is related to the presence of DSP or a sole function of specific surface area needs to be investigated in more detail. Fig. 8b illustrates a trend between workability and the measured BET surface of modified BR containing cements. The linear trend between the specific surface area and the ratio between added superplasticizer and mortar spread shows that the superplasticizer efficiency remains the same for the differently modified BRs. This means that no BR specific sorption effects of the superplasticizer (Master Glenium ACE 460) have to be considered while optimizing concrete rheology. The same trends as for $LC^3$ systems could be observed. Furthermore, no flash setting was observed, which makes the use of retarders optional. The BR induced increase in paste stiffness makes these binders suitable for additive manufacturing and material minimized construction as implied by the results of Zhang et al. on a quaternary blended cement containing iron tailings, BR, fly ash and OPC [236].

Most authors confirm that the addition of PCE-based superplasticizers is effective and allows the production of sufficiently flowable mortars and concretes for blended cements containing 10 to 40 wt% BR [36,234,237,238]. The impact of soluble sodium on workability was shown by Senff et al., who added not filter-pressed BR slurry to mortar. In comparison to filter pressed BRs significantly higher amounts of SP were needed to reach an equivalent increase of the flow value between 180 and 250 mm, due to the much higher contents of soluble sodium [38].

#### 5.1.2. Strength development

Most used concrete does not fully utilize the strength potential of the cement, since the most common strength classes found in structural applications range between C20/25 and C40/45. Blended cement with relative strengths (strength activity indices) $> 0.8$ usually can fulfil these criteria at 28 d if a common OPC is blended with the SCM. Fig. 8 compares the compressive strength of several BR-containing mortars with other blended cements. To ensure a comparability the absolute values are normalized by the strength of the used OPC references. The mortars have been made at a w/b ratio of 0.5 and without the use of SPs.

As seen in Fig. 8, BR containing cements (>10 wt% replacement) show a reduced 28d strength in comparison to OPC. Untreated BR have similar performance to limestone after 28 days, but can have higher strength at early age. This is an unusual behaviour for blended cements. An addition of >20 wt% untreated BR leads to a significant performance loss (SAI 0.5–0.6). In addition, this leads to strength loss at late age [38]. This is a common effect of too high alkali contents [38,165]. The impact of the SCM on early-hydration is related to an acceleration of the clinker's silicate reaction, due to the increased alkali content of the binder. However the alkali acceleration leads to a lower late age strength observed in high alkali cements [218,245]. The accelerated reaction is mainly related to the alkali induced pH increase and subsequently accelerated dissolution of $C_2S$ and $C_3S$ leading to a quicker C-S-H formation [190]. While an effect of high alkali concentration on C-S-H morphology, caused by a decrease of Ca/Si ratio, an increased Na or K/Si ratio and increased aluminate content have been reported [189,246], scientists still discuss the relevance of these findings for the macroscopic performance of alkali rich cements. One hypothesis states that differing C-A-S-H morphologies and compositions cause a reduced late age strength [201,247], while e.g. Zhang et al. argue that the increased ionic

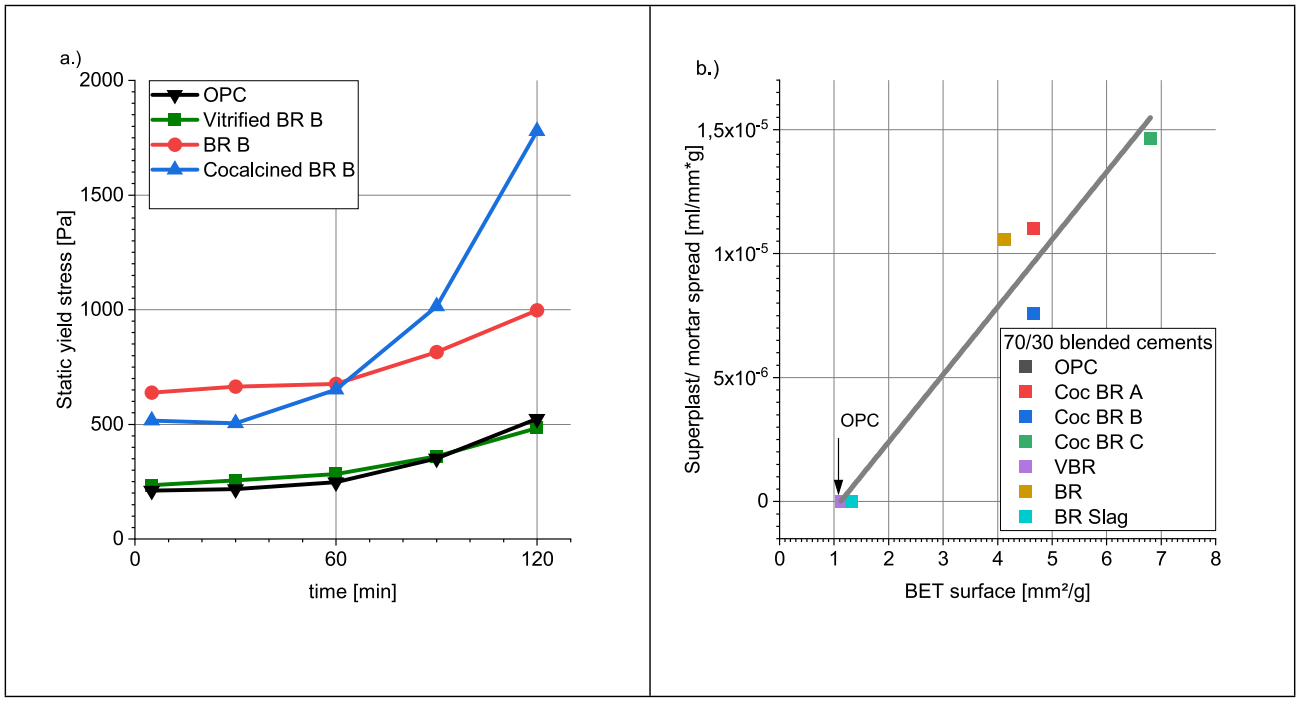


**Fig. 7.** (a) Development of static yield stress for differently treated BR. (b) Impact of specific surface area on workability for several BR-containing mortars (both own results).

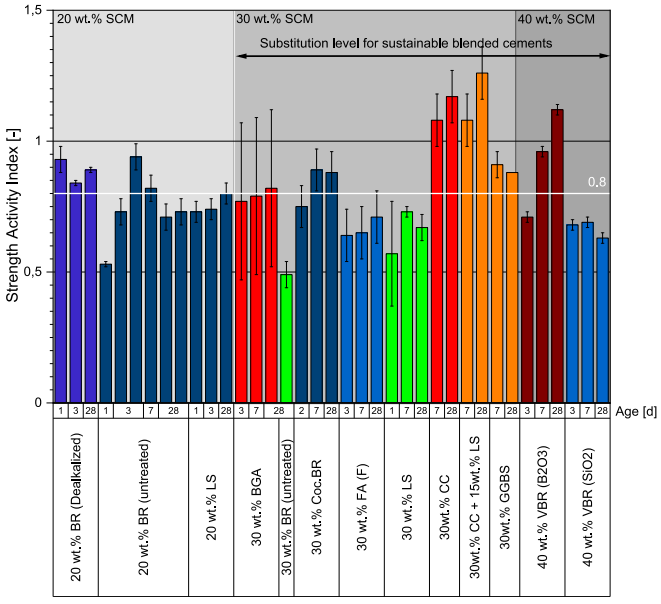


**Fig. 8.** Selected blended cements in comparison to BR addition between 20 and 40 wt%. The variance was either taken from the source publication or estimated by averaging the standard deviations of SAIs of systems containing between 20 and 40 wt% SCM [28,29,31,54,94,204–220].

strength of the alkali-rich pore solution leads to a decrease in water activity and an increase in self-desiccation, which stops the hydration reactions [203]. How soluble alkalis affect the reactivity of various SCMs needs to be investigated in more detail.

A reduced 28 d strength is common for pozzolanic SCMs like FA. They usually give their contribution to strength at late ages. Chemically modified BRs can reach SAIs (according to EN) of 0.8 putting them in a range similar to other pozzolanic SCMs (see Fig. 8) [36,173,220,239]. The contribution of co-calcined BR with clay to hydration leads to an SAI above 0.8 at 7 d, which is rather high for a blended cement containing 30 wt% of pozzolan [36]. BR based slags can be used at replacement levels of up to 40 wt% and reach SAIs >0.8 at 28 d. This is confirmed by Bullerjahn and Mehringskötter [220]. In case of modified BR an alkali induced strength, loss was not reported, indicating a reduced Na solubility. In case of BR based slags a synergetic effect of limestone addition, similar to $LC^3$ systems, has been reported [220]. Modified BR blended cements reach a mechanical performance comparable to FA type F or low grade calcined clays [36,95]. As $R^3$ results (Fig. 6) suggest the 28 d strengths most likely depict the final strength of BR blended cements. Nevertheless, long-term experiments are needed to ensure that (modified) BRs do not lead to internal durability issues in blended cements.

The mortar results are confirmed in the concrete scale, where promising results could be obtained with correct mix-designs [57,146,232,237,238]. While these mix designs vary drastically, they show that BR containing binders are versatile enough to be used in structural concretes. It is expected to hold true for modified BRs, where concrete scaled data need to be generated. Nikbin et al. report that SCM rich (25 wt% BR) blended cements do cause an increased water demand similar to calcined clay systems. Similar results have been obtained by other researchers for standard [238,248] and self-compacting concretes [238,249–251]. A more detailed discussion of the impact of BR addition on the mechanical properties (e.g. flexural/splitting compressive strengths) of concretes is given in the review of Salim et al. [252].

### 5.1.3. *Shrinkage*

Silveira et al. provide chemical shrinkage data according to ASTM C-1608-17 for up to 20 wt% BR containing cement (Brazilian GGBFS cement) paste. The addition of LS and BR (20 wt%) almost doubled the chemical shrinkage to 0.067 ml/$g_{solid}$ after 48 h. In the investigated systems BR addition leads to a linear increase of chemical shrinkage [253]. This can be explained by the alkali-driven acceleration of silicate and aluminate reaction. Time-resolved shrinkage measurements correlate well with recorded calorimetry curves [253]. Higher pH and ion concentrations also increase the pore solutions' surface tension and increase capillary stresses [254,255], especially in shrinkage relevant gel- and capillary pore fractions.

Senff et al. show that BR addition increases drying shrinkage. They report values of up to 1.73 mm/m for 20 wt% replacement and 56 d storage according to EN 12390-16 and w/b values of approx. 0.5 [38]. This value is larger than the common range (0.4–0.8 mm/m) measured in cement-rich concretes and mortars. Table 11 (supplementary material) tries to provide an overview of the drying shrinkage of blended cement pastes. It can be seen (Fig. 9) that BR addition can also lead to drying shrinkage values comparable to applied systems. Some authors report a reduction of drying shrinkage with increasing BR addition. These data have been either taken on non-Bayer residue [249] or on ternary systems including BR and slags or silica fume [256,257,258]. No data was found for modified BRs. Data on the drying, autogenous and chemical shrinkage of these systems is needed to identify the different contributions to the total shrinkage, evaluate the efficiency of shrinkage reducing agents and verify the soundness of BR blended cements.

## 5.2. Durability

### 5.2.1. Moisture and water transport

Similar to other SCMs with high specific surface areas, like calcined clays of silica fume, BR has been reported to increase the water absorption at early ages [57]. Differences in aggregate composition, w/b-ratio and other not BR related mix-design parameters, as well as different experimental setups lead to a large variability of the present data.

Most researchers observed increased water absorption capacities between 5 and 30 wt% [38,57,146,251], while other researchers [102,232,259,260] observed a significant reduction in the water absorption capacity with increasing BR addition.

Above 30 wt% BR content only an increase in water absorption capacity was reported by Senff et al. [38]. BR addition could increase water absorption, due to the porosity and very high specific surface area of the BR particles. At lower replacement levels this effect could be insignificant in comparison to an optimized PSD of the binder, due to the very low particle sizes of BR.

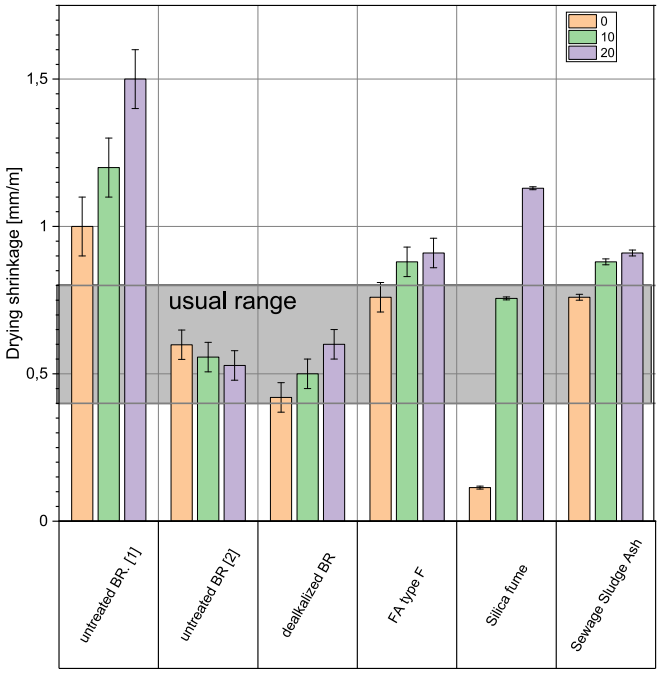


**Fig. 9.** Impression of the impact of BR and other pozzolanic SCMs on drying shrinkage (sample age 56 d stored at RH 65%, 20 °C). A more extensive data collection is included in the supplementary material (Table 11). Standard mortars (EN 196-1) at w/b = 0.50 ± 0.02 are compared in this figure. Only [249] was stored at RH 55 %. The shrinkage is calculated as defined in EN 12390-16 (a positive shrinkage means the sample gets smaller).
The data are replotted from [30,132,224,233–235].

Water sorptivity experiments indicate a complex effect of BR addition. Raja et al. could show that, in their binder system, a minimum of water sorptivity could be reached at 6 wt% BR addition. They confirmed this at multiple w/b-ratios, which suggests that the PSD of the used binders is mainly responsible for the differences between their samples [261]. In the case of equivalent mix-designs (same aggregate composition, workability, water content, etc.) several researchers observed significantly reduced sorptivities of BR containing concretes in time frames between hours to 150 d [102,237,261].

### 5.2.2. Carbonation

Senff et al. showed that BR addition increases carbonation velocity similar to a common pozzolan for two w/b ratios (0.47 and 0.58) on mortar. Their experiments were solely based on the phenolphthalein test after accelerated carbonation (0.2 bar $CO_2$ partial pressure) and covered binders with up to 40 wt% BR [38]. This is related to its pozzolanic reactivity and hence a reduced $Ca(OH)_2$ buffering capacity. Further detailed and systematic investigations, in particular on the effect of carbonation on the microstructure and transport properties of BR-containing cements, are missing.

Some information can be gathered from the context of BR neutralization, as described in Section 4.3.2. Cooling et al. showed that untreated BR forms dawsonite ($NaAlCO_3$) as well as X-ray amorphous sodium carbonate [123,227]. These should be the only BR-specific carbonate phases that differentiate BR containing blended cements from other Portland cement systems. A good review of the carbonation mechanisms in blended cements and the related challenges is given in [262].

### 5.2.3. Chloride ingress

Several authors [102,237,263] reported a positive impact of BR on chloride ingress resistance. The experiments have always been carried out in the concrete or mortar scale. To assess the influence of a material on chloride-induced rebar corrosion the chloride ingress, as well as the influence of the cements' pore solution on the corrosion rate of the rebar are needed [261,263]. The experiments of Venkantesh et al. and others uniformly show that BR addition (up to 20 wt%) has a positive impact on the corrosion resistance of rebars [237,260,261,263]. This could be related to the high pH of the BR blended cements pore solution (formation of the rebars passivation layer) and a reduced chloride ingress velocity.

The Rapid Chloride Penetration Test (RCPT, ASTM C 1202) was used for the characterization of BR-containing concretes. While giving a reliable comparison [265] this test does not yield a diffusion coefficient for use in models, which explains the need for other standards leading to stationary and non-stationary migration (NT build 492) tests. Fig. 10 shows the beneficial impact of BR addition on chloride transport as reported by Raja et al. [261].

Similarly, the data collected in Fig. 11 (Supplementary Table 10) show that BR addition improves Cl ingress resistance like other pozzolanic SCMs [232,237,243,261]. Ribeiro and Venkantesh suggest [237,264] that this improvement is mainly related to the PSD optimization (more fine particles) of the binder. The impact of thermochemically modified BRs on chloride binding and chloride transport properties has not yet been reported. Fig. 11 gives a representative selection of chloride ingress related durability data and shows that BR-based binders are promising for applications in chloride rich environments, since they perform similar to fly ash and slag containing cements.

To our knowledge, there was no detailed study on the mechanisms of the lower rate of chloride ingress due to the BR addition. BR-based composite cements have some properties that could lead to unusual characteristics in chloride binding. They combine an elevated pH with pozzolanic reactivity and a lower diffusion coefficient (compared to OPC) [237,264]. The pore solution pH influences all binding

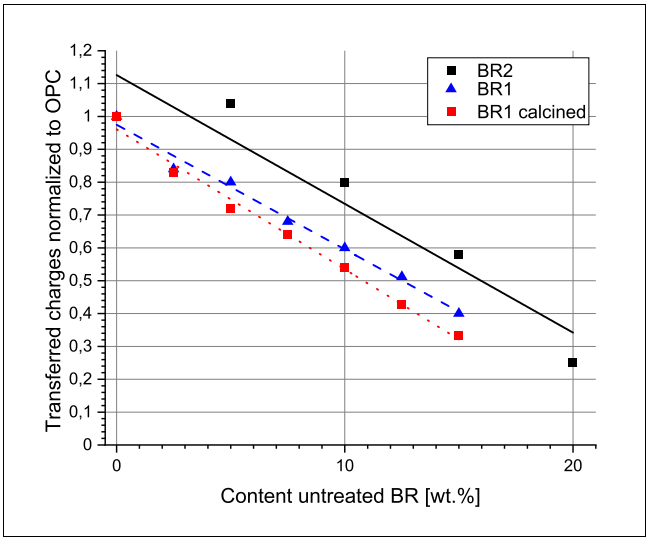


**Fig. 10.** Influence of BR content on the transferred charges [261].

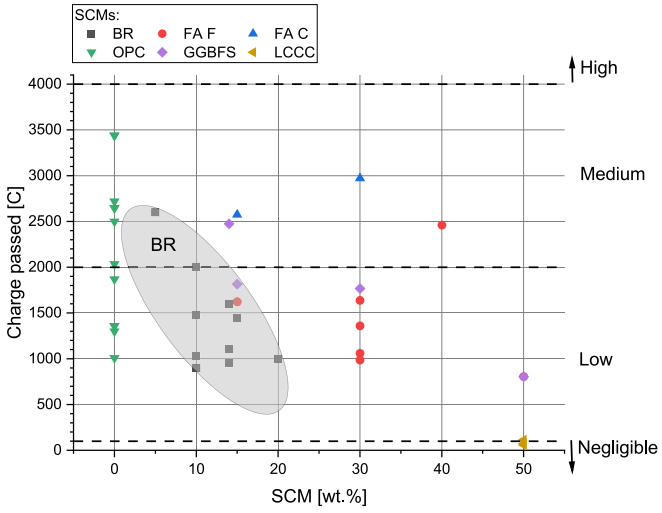


**Fig. 11.** Selected results of RCPT test after 28 d of sample curing. Data taken from [238,240–242].

mechanisms, and an overall decrease in binding capacity is expected for BR blended cements [225]. However, it is typically observed that diffusion coefficients are the dominant parameters for evaluating the resistance towards chloride induced rebar corrosion resistance [266].

### 5.2.4. External sulfate attack

Barbhuiya et al. showed that seawater-neutralized BR leads to an increased strength loss after 180 d in $MgSO_4$ solution [146]. Ghalehnovi et al. also showed that the presence of BR increased the sulfuric acid attack of concretes [251]. No contradicting results have been published.

Ignoring biogenic sulfuric acid corrosion and coupled durability issues, the main deterioration mechanisms are linked to the precipitation of sulfate rich phases in the solid structure. The created stresses then lead to cracking and the physical disintegration of the material [267]. Ettringite precipitation based on the reaction of AFm, CH and sulfate is observed. Furthermore gypsum and alkali sulfate precipitation can occur at very high sulfate concentrations (10 mmol/l) or cycle-based exposure [268]. It was shown that the supersaturation of the pore solution governs the expansion and damage by ettringite [269], because the supersaturation correlates with the maximum crystallization pressure and hence, the minimum pore-size in which ettringite crystals can nucleate. The smaller this diameter is, the higher the induced crystallization pressure, which leads to an increase in the macroscopic deterioration of the material. Due to the high alkali content of the BR, the pore solution of BR-containing cement is unique, which makes a more detailed analysis of this system necessary. Due to the known effects of elevated alkali contents on total and capillary porosity [270], physical sulfate attack also should be tested to evaluate the influence of capillary suction on the damage progression in real-world scenarios [268].

### 5.2.5. Alkali silica reaction

Alkali silica reactions (ASR) only occur in the presence of alkali-sensitive aggregates (which contain larger amounts of amorphous $SiO_2$) and a sufficiently high alkali content of the pore solution. A good insight into ASR mechanisms and studies is given by Thomas [271].

For BR-containing cements, an increase in the total alkali content of the pore solution (PS) can be assumed, due to the sodium-rich DSP (see Sections 2 to 3). An ASR performance similar to OPC (accelerated test according to NBR 14477-5) for blended cements containing 10–30 wt% of BR could be shown by Moraes Neves et al. [272]. The key difference was a quicker initial expansion, due to the increased sodium levels in the BR blended cements. Pore solution data for these systems are missing, so it cannot be clarified if an increased shrinkage counteracts the ASR based expansion, or if the deterioration is mitigated through the pore solution chemistry. Elevated concentrations of silicate and aluminate in the pore solution (caused by higher pH) should have a mitigating effect on the ASR in BR containing binders. The amount and nature of the DSP should be the determining factor for this effect. Hong and Glasser were the first to show that C-A-S-H phases have higher alkali binding capacities than C-S-H, which explains e.g. the increased ASR performance of calcined clay limestone cements [273,274]. Bhatty and Greening noticed the same effect in pozzolanic C-S-H with lower Ca/Si ratios [275].

Thermal treatments reduce the alkali release but still lead to much higher soluble sodium contents than in common blended cements [244]. The elevated alkali concentrations could reduce ASR resistance.

The ASR assessments of vitrified BR containing alkali activated cements published by Giels et al. show a promising performance [173]. Data of non-alkali activated binders containing at least 30 wt% BR based SCM are not available.

## 6. Conclusions

The Bayer process generates an unused waste stream of >170 Mt/a. The size of the waste stream limits a complete BR valorisation to soil amelioration and its inclusion in construction materials. An increasing shortage of FA and GGBS (in Europe), as well as the key position of SCMs in the cement industries sustainability strategy, lead to an interest in metallurgy wastes like BR.

Bayer BR is the insoluble residue of alkaline bauxite leaching. From a cement chemistry perspective this results in a high content (>50 wt%) of insoluble oxides, hydroxides and high sodium contents. BRs show a significant variation in chemical composition, amorphous content and mineralogy.

The (low) pozzolanic reactivity of BRs in cementitious systems, is based on sodium aluminosilicates (mainly sodalites and/or cancrinites). The increased formation of C-A-S-H, AFm and AFt was assumed in literature, but not investigated with systematic hydration studies. The thermodynamic simulation of the reaction of sodalite (the main DSP phase of gibbsitic BR) with portlandite and gypsum showed that the aforementioned phases are formed under conditions similar to a blended cement. This confirms the macroscopic observation that the Na contents of BR are not generally detrimental for the late age phase assemblage of blended cements. Hydration studies are needed to quantify reactivity and sulfate demand of BR blended cements. A final goal would be the development of fitting material models allowing a systematic optimization of microstructural characteristics and macroscopic performance.

This would be necessary to evaluate for which applications BR containing concretes can be used and which service lives can be assumed.

Main challenges of low clinker cements are early age strength development, reduced late age strength and reduced performance in some durability scenarios (e.g. carbonation). In the case of BR, activation treatments are needed to reach competitive substitution levels above 20 wt% and maintain sufficient relative strengths. Promising approaches are based on (1) ternary blended cements mixing >10 wt% BR with >20 wt% of pozzolanic or latent hydraulic SCMs, (2) thermal activation of BR in the presence of other pozzolans and (3) the formation of BR containing slags. Such materials have been synthesized in lab scale and yield pozzolanic reactivities comparable to FA and GGBFS. The elevated Na content of all BR based SCMs leads to a slight alkali acceleration of the system, which is beneficial for the early age properties. To evaluate the ecologic and economic impact of these BR utilization pathways LCA studies have to be conducted. For BR activation technologies no data from industrial pilot trials are available, which makes a proper sustainability assessment of the modified SCMs impossible.

Data regarding the long-term performance of BR containing binders with an SCM content of 20–50 wt% are scarce. This is also true for the impact of BR addition on some durability issues. It has been reported that BR addition leads to reduced late age strength, lowered $Cl^-$ diffusivities and increased carbonation velocity. An increased drying and chemical shrinkage with BR addition could be observed in some cases, while other researchers report a positive impact on drying shrinkage. These are common characteristics for pozzolan containing cements.

The sensitivity of BR containing cements towards ASR and external sulfate attack has not been reported sufficiently. If BR, especially in a modified form, is to be used as an SCM, comprehensive durability assessments of these materials are needed to define fitting applications. It is especially important to include common blended cements as references, because they are the benchmark that has to be met. Quantitative information regarding long term phase assemblage, engineering and durability performance are key-elements towards evaluating the economic and environmental impact of BR containing cements with 30–50 wt% substitution level.

## CRediT authorship contribution statement

**Michael Wenzel:** Writing – original draft, Visualization, Formal analysis, Data curation, Conceptualization. **Fabien Georget:** Writing – review & editing, Supervision, Project administration. **Thomas Matschei:** Validation, Supervision, Funding acquisition.

## Declaration of Generative AI and AI-assisted technologies in the writing process

During the preparation of this work the author(s) used Grammarly in order to correct grammar and optimize the wording of the article. No generative KI features were used. After using this tool, the author(s) reviewed and edited the content as needed and take full responsibility for the content of the publication.

## Declaration of competing interest

The authors declare that they have no known competing financial interests or personal relationships that could have appeared to influence the work reported in this paper.

## Acknowledgements

This research was carried out in the framework of the ReActiv project. It was completely funded by the EUs Horizon 2020 programme (Grant Agreement 958208). The authors are grateful for the constructive comments of the research consortium members and the contribution of Ken Evans and Efthymios Balomenos. Their insights in the alumina industry were valuable for the first part of the review. Furthermore, we thank the Holcim Innovation Center for supplying the materials needed for this study.

## Appendix A. Supplementary data

Supplementary data to this article can be found online at https://doi.org/10.1016/j.cemconres.2025.107854.

## Data availability

The analyzed data are included in the supplementary material.

## References

[1] H. Ostovari, L. Müller, J. Skocek, und A. Bardow, „From unavoidable $CO_2$ source to $CO_2$ sink? A cement industry based on $CO_2$ mineralization“, Environ. Sci. Technol., Bd. 55, Nr. 8, S. 5212–5223, Apr. 2021, doi: https://doi.org/10.1021/acs.est.0c07599.

[2] F.N. Stafford, A.C. Dias, L. Arroja, J.A. Labrincha, D. Hotza, Life cycle assessment of the production of Portland cement: a Southern Europe case study, J. Clean. Prod. 126 (July 2016) 159–165, https://doi.org/10.1016/j.jclepro.2016.02.110.

[3] A. Josa, A. Aguado, A. Heino, E. Byars, und A. Cardim, „Comparative analysis of available life cycle inventories of cement in the EU“, Cem. Concr. Res., Bd. 34, Nr. 8, S. 1313–1320, Aug. 2004, doi: https://doi.org/10.1016/j.cemconres.2003.12.020.

[4] D.A. Salas, A.D. Ramirez, C.R. Rodríguez, D.M. Petroche, A.J. Boero, J. Duque-Rivera, Environmental impacts, life cycle assessment and potential improvement measures for cement production: a literature review, J. Clean. Prod. 113 (Feb. 2016) 114–122, https://doi.org/10.1016/j.jclepro.2015.11.078.

[5] W. Shanks, C.F. Dunant, M.P. Drewniok, R.C. Lupton, A. Serrenho, J.M. Allwood, How much cement can we do without? Lessons from cement material flows in the UK, Resour. Conserv. Recycl. 141 (Feb. 2019) 441–454, https://doi.org/10.1016/j.resconrec.2018.11. 002.

[6] N.A. Madlool, R. Saidur, M.S. Hossain, N.A. Rahim, A critical review on energy use and savings in the cement industries, Renew. Sust. Energ. Rev. 15, Nr. 4 (May 2011) 2042–2060, https://doi.org/10.1016/j.rser.2011.01.005.

[7] S. Pamenter und R. J. Myers, „Decarbonizing the cementitious materials cycle: a whole-systems review of measures to decarbonize the cement supply chain in the UK and European contexts“, J. Ind. Ecol., Bd. 25, Nr. 2, S. 359–376, Apr. 2021, doi: https://doi.org/10.1111/jiec.13105.

[8] M. Kazemian, S. Sedighi, A. A. Ramezanianpour, F. Bahman-Zadeh, und A. M. Ramezanianpour, „Effects of cyclic carbonation and chloride ingress on durability properties of mortars containing Trass and Pumice natural pozzolans“, Struct. Concr., Bd. 22, Nr. 5, S. 2704–2719, Oct. 2021, doi: https://doi.org/10.1002/suco.201900529.

[9] P.N. Lemougna, et al., Review on the use of volcanic ashes for engineering applications, Resour. Conserv. Recycl. 137 (Oct. 2018) 177–190, https://doi.org/10.1016/j.resconrec.2018.05.031.

[10] K. Kupwade-Patil, S. Chin, J. Ilavsky, R. N. Andrews, A. Bumajdad, und O. Büyüköztürk, „Hydration kinetics and morphology of cement pastes with pozzolanic volcanic ash studied via synchrotron-based techniques“, J. Mater. Sci., Bd. 53, Nr. 3, S. 1743–1757, Feb. 2018, doi: https://doi.org/10.1007/s10853-017-1659-4.

[11] H. Olmez und E. Erdem, „The effects of phosphogypsum on the setting and mechanical properties of Portland cement and trass cement“, Cement Concr. Res. Bd. 19, Nr. 3, S. 8.

[12] K. Scrivener, F. Martirena, S. Bishnoi, S. Maity, Calcined clay limestone cements (LC3), Cem. Concr. Res. 114 (2018) 49–56, https://doi.org/10.1016/j.cemconres.2017. 08.017.

[13] V. Shah, A. Parashar, G. Mishra, S. Medepalli, S. Krishnan, und S. Bishnoi, „Influence of cement replacement by limestone calcined clay pozzolan on the engineering properties of mortar and concrete“, Adv. Cem. Res., Bd. 32, Nr. 3, S. 101–111, 2020, doi: https://doi.org/10.1680/jadcr.18.00073.

[14] G. Qiu, Z. Luo, Z. Shi, und M. Ni, „Utilization of coal gangue and copper tailings as clay for cement clinker calcinations“, J. Wuhan Univ. Technol. Mater. Sci. Ed., Bd. 26, Nr. 6, S. 1205–1210, Dec. 2011, doi: https://doi.org/10.1007/s11595-011-0391-1.

[15] F. Vargas, M. Lopez, Development of a new supplementary cementitious material from the activation of copper tailings: mechanical performance and analysis of factors, J. Clean. Prod. 182 (2018) 427–436, https://doi.org/10.1016/j.jclepro.2018.01.223.

[16] M. Schneider, M. Romer, M. Tschudin, und H. Bolio, „Sustainable cement production—present and future“, Cement Concr. Res., Bd. 41, Nr. 7, S. 642–650, July 2011, doi: https://doi.org/10.1016/j.cemconres.2011.03.019.

[17] K. Evans, „The history, challenges, and new developments in the management and use of bauxite residue“, J. Sustain. Metall., Bd. 2, Nr. 4, S. 316–331, Dec. 2016, doi: https://doi.org/10.1007/s40831-016-0060-x.

[18] D. V. Ribeiro, J. A. Labrincha, und M. R. Morelli, „Potential use of natural red mud as pozzolan for Portland cement“, Mater. Res., Bd. 14, Nr. 1, S. 60–66, Jan. 2011, doi: https://doi.org/10.1590/S1516-14392011005000001.

[19] Y. Pontikes, G.N. Angelopoulos, Bauxite residue in cement and cementitious applications: current status and a possible way forward, Resour. Conserv. Recycl. 73 (Apr. 2013) 53–63, https://doi.org/10.1016/j.resconrec.2013.01.005.

[20] Internation Aluminium, Statistic data of annual alumina production of International Aluminium members, Statistics Alumina production. [Online]. Verfügbar unter: https://international-aluminium.org/statistics/alumina-production/.

[21] A. Ruys, 3 — Refining of alumina: the Bayer process, in: A. Ruys (Ed.), Alumina Ceramics, Woodhead Publishing, 2019, pp. 49–70, https://doi.org/10.1016/B978-0-08-102442-3.00003-8.

[22] M.K. Kar, M.A.R. Önal, C.R. Borra, Alumina recovery from bauxite residue: a concise review, Resour. Conserv. Recycl. 198 (Nov. 2023) 107158, https://doi.org/10.1016/j.resconrec.2023.107158.

[23] M.C.G. Juenger, R. Snellings, S.A. Bernal, Supplementary cementitious materials: new sources, characterization, and performance insights, Cem. Concr. Res. 122 (Aug. 2019) 257–273, https://doi.org/10.1016/j.cemconres.2019.05.008.

[24] International Aluminium Institute, Maximising the use of bauxite residue in cement, in: Technology Roadmap, 1st ed., Nov. 2020. Zugegriffen: 3. März 2023. [Online]. Verfügbar unter: https://international-aluminium.org/resource/technology-roadmap-maximizing-the-use-of-bauxite-residue-in-cement/.

[25] X. Le Den, M. Caspani, N. Bey, C. Marton, K. Sveistrup Holck, N. Janin Mayr, NET-ZERO by 2050: Science-based Decarbonisation Pathways for the European Aluminium Industry, European Aluminium, November 2023. Zugegriffen: 11. April 2024. [Online]. Verfügbar unter: https://european-aluminium.eu/wp-content/uploads/2023/11/23-11-14-Net-Zero-by-2050-Science-based-Decarbonisation-Pathways-for-the-European-Aluminium-Industry_FULL-REPORT.pdf.

[26] R. Snellings, Assessing, understanding and unlocking supplementary cementitious materials, RILEM Techn. Lett. 1 (2016) 50–55.

[27] I. H. Shah, S. A. Miller, D. Jiang, und R. J. Myers, „Cement substitution with secondary materials can reduce annual global $CO_2$ emissions by up to 1.3 gigatons“, Nat. Commun., Bd. 13, Nr. 1, S. 5758, 2022.

[28] E. Aprianti, A huge number of artificial waste material can be supplementary cementitious material (SCM) for concrete production—a review part II, J. Clean. Prod. 142 (2017) 4178–4194.

[29] R. Snellings, P. Suraneni, J. Skibsted, Future and emerging supplementary cementitious materials, Cement Concr. Res. 171 (Sep. 2023) 107199, https://doi.org/10.1016/j.cemconres.2023.107199.

[30] M. Gräfe, G. Power, und C. Klauber, „Bauxite residue issues: III. Alkalinity and associated chemistry“, Hydrometallurgy, Bd. 108, Nr. 1–2, S. 60–79, June 2011, doi: https://doi.org/10.1016/j.hydromet.2011.02.004.

[31] E. Balomenos, et al., Bauxite residue (BR) producted by alumina refineries in Europe, Removal. Zugegriffen: 21. Juni 2022. [Online]. Verfügbar unter: https://www.spire2030.eu/sites/default/files/users/user740/removal_policy_brief_sep_2019.pdf, Sep. 2019.

[32] S.M.A. Qaidi, B.A. Tayeh, H.F. Isleem, A.R.G. de Azevedo, H.U. Ahmed, W. Emad, Sustainable utilization of red mud waste (bauxite residue) and slag for the production of geopolymer composites: a review, Case Stud. Construct. Mater. 16 (2022) e00994, https://doi.org/10.1016/j.cscm.2022.e00994.

[33] J. Yang, et al., A method and product for making geopolymer cementitious material from bauxite residue, CN103964710B. Zugegriffen: 11. Mai 2022. [Online]. Verfügbar unter: https://patents.google.com/patent/CN103964710B/en?oq=Geopolymer+bauxite+residue, 28. Januar 2015.

[34] M. D. Kamitsou, D. G. Kanellopoulou, A. Christogerou, C. Kostagiannakopoulou, V. Kostopoulos, und G. N. Angelopoulos, „Valorization of FGD and bauxite residue in sulfobelite cement production“, Waste Biomass Valor., Bd. 11, Nr. 10, S. 5445–5456, Oct. 2020, doi: https://doi.org/10.1007/s12649-020-01055-9.

[35] T. Danner und H. Justnes, „Bauxite residue as supplementary cementitious material — efforts to reduce the amount of soluble sodium“, Nord. Concr. Res., Bd. 62, Nr. 1, S. 1–20, June 2020, doi: https://doi.org/10.2478/ncr-2020-0001.

[36] A. Peys, T. Hertel, und R. Snellings, „Co-calcination of bauxite residue with kaolinite in pursuit of a robust and high-quality supplementary cementitious material“, Frontiers in Materials, S. 384.

[37] F. Bullerjahn, G. Bolte, Composition of the reactivity of engineered slags from bauxite residue and steel slag smelting and use as SCM for Portland cement, Constr. Build. Mater. 321 (2022) 126331.

[38] L. Senff, R.C.E. Modolo, A.S. Silva, V.M. Ferreira, D. Hotza, J.A. Labrincha, Influence of red mud addition on rheological behavior and hardened properties of mortars, Constr. Build. Mater. 65 (Aug. 2014) 84–91, https://doi.org/10.1016/j.conbuildmat.2014.04.104.

[39] D. V. Ribeiro, A. S. Silva, J. A. Labrincha, und M. R. Morelli, „Rheological properties and hydration behavior of Portland cement mortars containing calcined red mud“, Can. J. Civ. Eng., Bd. 40, Nr. 6, S. 557–566, 2013, doi: https://doi.org/10.1139/cjce-2012-0230.

[40] A. Goronovski, R.M. Rivera, T. Van Gerven, A.H. Tkaczyk, Radiological assessment of bauxite residue processing to enable zero-waste valorisation and regulatory compliance, J. Clean. Prod. 294 (Apr. 2021) 125165, https://doi.org/10.1016/j.jclepro.2020.125165.

[41] C. M. Carter, H. A. van der Sloot, D. Cooling, A. van Zomeren, und T. Matheson, „Characterization of untreated and neutralized bauxite residue for improved waste management“, Environ. Eng. Sci., Bd. 25, Nr. 4, S. 475–488, 2008.

[42] M.A. Khairul, J. Zanganeh, B. Moghtaderi, The composition, recycling and utilisation of Bayer red mud, Resour. Conserv. Recycl. 141 (2019) 483–498, https://doi.org/10.1016/j.resconrec.2018.11.006.

[43] F. Lyu, Y. Hu, L. Wang, W. Sun, Dealkalization processes of bauxite residue: a comprehensive review, J. Hazard. Mater. 403 (Feb. 2021) 123671, https://doi.org/10.1016/j.jhazmat.2020.123671.

[44] F. M. Kaußen und B. Friedrich, „Methods for alkaline recovery of aluminum from bauxite residue“, J. Sustain. Metall., Bd. 2, Nr. 4, S. 353–364, Dec. 2016, doi: https://doi.org/10.1007/s40831-016-0059-3.

[45] H.Y. Yu, X.L. Pan, K.W. Dong, W. Zhang, S.W. Bi, The sintering and leaching of low-grade diasporic bauxite by the improved lime-sintering process, AMR 616–618 (Dec. 2012) 1051–1054, https://doi.org/10.4028/www.scientific.net/AMR.616-618.1051.

[46] V. Smirnov, „Alumina production in Russia part I: historical background“, JOM, Bd. 48, Nr. 8, S. 24–26, Aug. 1996, doi: https://doi.org/10.1007/BF03223020.

[47] X. Liu, N. Zhang, Y. Yao, H. Sun, H. Feng, Micro-structural characterization of the hydration products of bauxite-calcination-method red mud-coal gangue based cementitious materials, J. Hazard. Mater. 262 (Nov. 2013) 428–438, https://doi.org/10.1016/j.jhazmat.2013.08.078.

[48] F.G. Bell, Engineering Geology, Elsevier, 2007.

[49] W. Liu, J. Yang, und B. Xiao, „Review on treatment and utilization of bauxite residues in China“, Int. J. Miner. Process., Bd. 93, Nr. 3–4, S. 220–231, Dec. 2009, doi: https://doi.org/10.1016/j.minpro.2009.08.005.

[50] H. Strunz, E. Nickel, Strunz Mineralogical Tables. Chemical-structural Mineral Classification System, 9. Auflage., E. Scheizerbart'sche Verlagsbuchhandlung, Stuttgard, 2001, p. 239.

[51] Y. Li, X. Pan, Z. Lv, H. Wu, H. Yu, Multi-element comprehensive utilization of high-silicon bauxite by roasting pretreatment and two-stage leaching, Miner. Eng. 187 (Sep. 2022) 107805, https://doi.org/10.1016/j.mineng.2022.107805.

[52] W. Cao, W. Tian, Z. Hong, Study on Bayer Process and Soda-lime Sintering Process of Special Diasporic Bauxite With High Silica, Jan. 2010, pp. 149–153.

[53] A. R. Hind, S. K. Bhargava, und S. C. Grocott, „The surface chemistry of Bayer process solids: a review“, Colloids Surf. A Physicochem. Eng. Asp., Bd. 146, Nr. 1, S. 359–374, 1999, doi: https://doi.org/10.1016/S0927-7757(98)00798-5.

[54] R. Sonthalia, P. Behara, T. Kumaresan, S. Thakre, Review on alumina trihydrate precipitation mechanisms and effect of Bayer impurities on hydrate particle growth rate, International Journal of Mineral Processing 125 (Dec. 2013) 137–148, https://doi.org/10.1016/j.minpro.2013.08.002.

[55] G. Power, J. S. C. Loh, J. E. Wajon, F. Busetti, und C. Joll, „A review of the determination of organic compounds in Bayer process liquors“, Anal. Chim. Acta, Bd. 689, Nr. 1, S. 8–21, 2011, doi: https://doi.org/10.1016/j.aca.2011.01.040.

[56] A. Danaei, Fundamental Study of Red Mud Based Fluxes for Desulphurization and Dephosphorization of Hot Metal, 2015.

[57] I.M. Nikbin, M. Aliaghazadeh, Sh. Charkhtab, A. Fathollahpour, Environmental impacts and mechanical properties of lightweight concrete containing bauxite residue (red mud), J. Clean. Prod. 172 (Jan. 2018) 2683–2694, https://doi.org/10.1016/j.jclepro.2017.11.143.

[58] D. Herfort, B. Lothenbach, 11 Ternary phase diagrams applied to hydrated cement, in: A Ptractical Guide to Microstructural Analysis of Cementitious Materials, CRC Press Taylor & Francis Group, Boca Raton, FL, 2016, pp. 485–509.

[59] H.F.W. Taylor, Cement Chemistry, 2nd ed., T. Telford, London, 1997.

[60] E.S. Aprianti, A huge number of artificial waste material can be supplementary cementitious material (SCM) for concrete production — a review part II, J. Clean. Prod. 142 (Jan. 2017) 4178–4194, https://doi.org/10.1016/j.jclepro.2015.12.115.

[61] B. Ercikdi, F. Cihangir, A. Kesimal, H. Deveci, und İ. Alp, „Effect of natural pozzolans as mineral admixture on the performance of cemented-paste backfill of sulphide-rich tailings“, Waste Manag. Res., Bd. 28, Nr. 5, S. 430–435, May 2010, doi: https://doi.org/10.1177/0734242X09351905.

[62] M. Antoni, Investigation of cement substitution by blends of calcined clays and limestone, in: Monograph, École Polytechnique Fédérale de Lausanne, Lausanne, 2013, https://doi.org/10.5075/epfl-thesis-6001. Zugegriffen: 21. Dezember 2022. [Online]. Verfügbar unter:.

[63] F. Avet, K. Scrivener, Investigation of the calcined kaolinite content on the hydration of Limestone Calcined Clay Cement (LC3), Cem. Concr. Res. 107 (May 2018) 124–135, https://doi.org/10.1016/j.cemconres.2018.02.016.

[64] H. Wang, et al., Synergistic effects of supplementary cementitious materials in limestone and calcined clay-replaced slag cement, Constr. Build. Mater. 282 (May 2021) 122648, https://doi.org/10.1016/j.conbuildmat.2021.122648.

[65] N. Bouazza, A.E. Mrihi, A. Maâte, Geochemical assessment of limestone for cement manufacturing, Proc. Technol. 22 (2016) 211–218, https://doi.org/10.1016/j.protcy.2016.01.046.

[66] N. Garg, J. Skibsted, Pozzolanic reactivity of a calcined interstratified illite/smectite (70/30) clay, Cem. Concr. Res. 79 (Jan. 2016) 101–111, https://doi.org/10.1016/j.cemconres.2015.08.006.

[67] R. B. E. Boum et al., „Thermal behaviour of metakaolin–bauxite blends geopolymer: micro- structure and mechanical properties“, SN Appl. Sci., Bd. 2, Nr. 8, S. 1358, Aug. 2020, doi: https://doi.org/10.1007/s42452-020-3138-9.

[68] M.A. Villaquirán-Caicedo, Studying different silica sources for preparation of alternative waterglass used in preparation of binary geopolymer binders from metakaolin/boiler slag, Construct. Build. Mater. 227 (Dec. 2019) 116621, https://doi.org/10.1016/j.conbuild-mat.2019.08.002.

[69] Y. Cao, Y. Wang, Z. Zhang, Y. Ma, H. Wang, Recent progress of utilization of activated kaolinitic clay in cementitious construction materials, Compos. Pt. B Eng. 211 (Apr. 2021) 108636, https://doi.org/10.1016/j.compositesb.2021.108636.

[70] M.C.G. Juenger, R. Siddique, Recent advances in understanding the role of supplementary cementitious materials in concrete, Cem. Concr. Res. 78 (Dec. 2015) 71–80, https://doi.org/10.1016/j.cemconres.2015.03.018.

[71] W. A. Tasong, S. Wild, und R. J. D. Tilley, „Mechanisms by which ground granulated blast-furnace slag prevents sulphate attack of lime-stabilised

kaolinite“, Cem. Concr. Res., Bd. 29, Nr. 7, S. 975–982, July 1999, doi: https://doi.org/10.1016/S0008-8846(99)00007-1.
[72] A. Atasoy, „An investigation on characterization and thermal analysis of the Aughinish red mud“, J. Therm. Anal. Calorim., Bd. 81, Nr. 2, S. 357–361, July 2005, doi: https://doi.org/10.1007/s10973-005-0792-5.
[73] O.R. Ogirigbo, L. Black, Influence of slag composition and temperature on the hydration and microstructure of slag blended cements, Constr. Build. Mater. 126 (Nov. 2016) 496–507, https://doi.org/10.1016/j.conbuildmat.2016.09.057.
[74] S. Sasui, G. Kim, J. Nam, A. van Riessen, und M. Hadzima-Nyarko, „Effects of waste glass as a sand replacement on the strength and durability of fly ash/GGBS based alkali activated mortar“, Ceram. Int., Bd. 47, Nr. 15, S. 21175–21196, Aug. 2021, doi: https://doi.org/10.1016/j.ceramint.2021.04.121.
[75] M. O'Connell, C. McNally, und M. G. Richardson, „Performance of concrete incorporating GGBS in aggressive wastewater environments“, Constr. Build. Mater., Bd. 27, Nr. 1, S. 368–374, Feb. 2012, doi: https://doi.org/10.1016/j.conbuildmat.2011.07.036.
[76] A. Oner und S. Akyuz, „An experimental study on optimum usage of GGBS for the compressive strength of concrete“, Cem. Concr. Compos., Bd. 29, Nr. 6, S. 505–514, July 2007, doi: https://doi.org/10.1016/j.cemconcomp.2007.01.001.
[77] D. Glosser, A. Choudhary, O. B. Isgor, und W. J. Weiss, „Investigation of the reactivity of fly ash and its effect on mixture properties“, ACI Mater. J., Bd. 116, Nr. 4, July 2019, doi: 10.14359/51716722.
[78] M. H. Shehata und M. D. A. Thomas, „The effect of fly ash composition on the expansion of concrete due to alkali–silica reaction“, Cem. Concr. Res., Bd. 30, Nr. 7, S. 1063–1072, July 2000, doi: https://doi.org/10.1016/S0008-8846(00)00283-0.
[79] H. Yildirim, M. Sümer, V. Akyüncü, und E. Gürbüz, „Comparison on efficiency factors of F and C types of fly ashes“, Constr. Build. Mater., Bd. 25, Nr. 6, S. 2939–2947, June 2011, doi: https://doi.org/10.1016/j.conbuildmat.2010.12.009.
[80] T. Huang, B. Li, Q. Yuan, Z. Shi, Y. Xie, C. Shi, Rheological behavior of Portland clinker-calcium sulphoaluminate clinker-anhydrite ternary blend, Cem. Concr. Compos. 104 (Nov. 2019) 103403, https://doi.org/10.1016/j.cemconcomp.2019.103403.
[81] K. Scrivener, R. Snellings, B. Lothenbach, A Practical Guide to Microstructural Analysis of Cementitious Materials, 0 Aufl., CRC Press, 2018, https://doi.org/10.1201/b19074.
[82] W. Kunther, Z. Dai, J. Skibsted, Thermodynamic modeling of hydrated white Portland cement–metakaolin–limestone blends utilizing hydration kinetics from $^{29}$Si MAS NMR spectroscopy, Cem. Concr. Res. 86 (Aug. 2016) 29–41, https://doi.org/10.1016/j.cemconres.2016.04.012.
[83] J.J. Wolf, D. Jansen, F. Goetz-Neunhoeffer, J. Neubauer, Impact of varying $Li_2CO_3$ additions on the hydration of ternary CSA-OPC-anhydrite mixes, Cem. Concr. Res. 131 (May 2020) 106015, https://doi.org/10.1016/j.cemconres.2020.106015.
[84] F. Bertola, D. Gastaldi, S. Irico, G. Paul, F. Canonico, Behavior of blends of CSA and Portland cements in high chloride environment, Constr. Build. Mater. 262 (Nov. 2020) 120852, https://doi.org/10.1016/j.conbuildmat.2020.120852.
[85] C. Cau Dit Coumes, M. Dhoury, J.-B. Champenois, C. Mercier, D. Damidot, Physico-chemical mechanisms involved in the acceleration of the hydration of calcium sulfoaluminate cement by lithium ions, Cem. Concr. Res. 96 (June 2017) 42–51, https://doi.org/10.1016/j.cemconres.2017.03.004.
[86] J. Acordi, A. Luza, D.C.N. Fabris, F. Raupp-Pereira, A. De Noni Jr, O.R. K. Montedo, New waste-based supplementary cementitious materials: mortars and concrete formulations, Construct. Build. Mater. 240 (Apr. 2020) 117877, https://doi.org/10.1016/j.conbuild-mat.2019.117877.
[87] Z. Hussain et al., „Enhanced mechanical properties of wood ash and fly ash as supplementary cementitious materials“, Adv. Appl. Ceram., Bd. 116, Nr. 7, S. 355–361, Oct. 2017, doi: https://doi.org/10.1080/17436753.2017.1321274.
[88] A. Akkarapongtrakul, P. Julphunthong, und T. Nochaiya, „Setting time and microstructure of Portland cement-bottom ash–sugarcane bagasse ash pastes“, Monatsh. Chem., Bd. 148, Nr. 7, S. 1355–1362, July 2017, doi: https://doi.org/10.1007/s00706-017-1953-5.
[89] W. Ahmad, A. Ahmad, K.A. Ostrowski, F. Aslam, P. Joyklad, P. Zajdel, Sustainable approach of using sugarcane bagasse ash in cement-based composites: a systematic review, Case Stud. Construct. Mater. 15 (Dec. 2021) e00698, https://doi.org/10.1016/j.cscm.2021.e00698.
[90] S. O. Bamaga, M. W. Hussin, und M. A. Ismail, „Palm oil fuel ash: promising supplementary cementing materials“, KSCE J. Civ. Eng., Bd. 17, Nr. 7, S. 1708–1713, Nov. 2013, doi: https://doi.org/10.1007/s12205-013-1241-9.
[91] W. Kroehong, T. Sinsiri, C. Jaturapitakkul, und P. Chindaprasirt, „Effect of palm oil fuel ash fineness on the microstructure of blended cement paste“, Constr. Build. Mater., Bd. 25, Nr. 11, S. 4095–4104, Nov. 2011, doi: https://doi.org/10.1016/j.conbuildmat.2011.04.062.
[92] S.C. Taylor-Lange, E.L. Lamon, K.A. Riding, M.C.G. Juenger, Calcined kaolinite–bentonite clay blends as supplementary cementitious materials, Appl. Clay Sci. 108 (2015) 84–93, https://doi.org/10.1016/j.clay.2015.01.025.
[93] F. Avet, R. Snellings, A.A. Diaz, M.B. Haha, K. Scrivener, Development of a new rapid, relevant and reliable (R3) test method to evaluate the pozzolanic reactivity of calcined kaolinitic clays, Cem. Concr. Res. 85 (2016) 1–11.
[94] T. Danner, G. Norden, H. Justnes, Characterisation of calcined raw clays suitable as supplementary cementitious materials, Appl. Clay Sci. 162 (2018) 391–402, https://doi.org/10.1016/j.clay.2018.06.030.
[95] T. Hertel, A. Van den Bulck, B. Blanpain, Y. Pontikes, Correlating the amorphous phase structure of vitrified bauxite residue (red mud) to the initial reactivity in binder systems, Cement Concr. Compos. 127 (March 2022) 104410, https://doi.org/10.1016/j.cemcon-comp.2022.104410.
[96] P. S. Reddy et al., „Properties and assessment of applications of red mud (bauxite residue): current status and research needs“, Waste Biomass Valor., Bd. 12, Nr. 3, S. 1185–1217, March 2021, doi: https://doi.org/10.1007/s12649-020-01089-z.
[97] A. Kolencsik-Tóth et al., „Physical and Chemical Characterization of Red Mud in Terms of Its Environmental Effects“, S. 10.
[98] C.R. Borra, Y. Pontikes, K. Binnemans, T. Van Gerven, Leaching of rare earths from bauxite residue (red mud), Miner. Eng. 76 (May 2015) 20–27, https://doi.org/10.1016/j.mineng.2015.01.005.
[99] R.M. Rivera, G. Ounoughene, C.R. Borra, K. Binnemans, T. Van Gerven, Neutralisation of bauxite residue by carbon dioxide prior to acidic leaching for metal recovery, Miner. Eng. 112 (Oct. 2017) 92–102, https://doi.org/10.1016/j.mineng.2017.07.011.
[100] O. Canbek, S. Shakouri, S.T. Erdoğan, Laboratory production of calcium sulfoaluminate cements with high industrial waste content, Cem. Concr. Compos. 106 (Feb. 2020) 103475, https://doi.org/10.1016/j.cemconcomp.2019.103475.
[101] A. Alp, M.S. Goral, The Influence of Soda Additive on the Thermal Properties of Red Mud, 2003.
[102] C. Venkatesh, R. Nerella, und M. S. R. Chand, „Role of red mud as a cementing material in concrete: a comprehensive study on durability behavior“, Innov. Infrastruct. Solut., Bd. 6, Nr. 1, S. 13, March 2021, doi: https://doi.org/10.1007/s41062-020-00371-2.
[103] J. Yang und B. Xiao, „Development of unsintered construction materials from red mud wastes produced in the sintering alumina process“, Constr. Build. Mater., Bd. 22, Nr. 12, S. 2299–2307, Dec. 2008, doi: https://doi.org/10.1016/j.conbuildmat.2007.10.005.
[104] P.B. Cusack, R. Courtney, M.G. Healy, L.M.T.O. Donoghue, É. Ujaczki, An evaluation of the general composition and critical raw material content of bauxite residue in a storage area over a twelve-year period, J. Clean. Prod. 208 (2019) 393–401, https://doi.org/10.1016/j.jclepro.2018.10.083.
[105] H. Peng, J. Vaughan, S. Wang, J. Vogrin, D. Seneviratne, Chemical thermodynamics and reaction kinetics of Bayer process desilication, in: Gehalten auf der TMS Annual Meeting & Exhibition, Springer, 2024, pp. 3–12.
[106] A. Peys, et al., Sustainable iron-rich cements: raw material sources and binder types, Cem. Concr. Res. 157 (July 2022) 106834, https://doi.org/10.1016/j.cemconres.2022.106834.
[107] B.Z. Dilnesa, E. Wieland, B. Lothenbach, R. Dähn, K.L. Scrivener, Fe-containing phases in hydrated cements, Cem. Concr. Res. 58 (2014) 45–55, https://doi.org/10.1016/j.cemconres.2013.12.012.
[108] C. Siakati, A.P. Douvalis, V. Hallet, A. Peys, Y. Pontikes, Influence of CaO/FeO ratio on the formation mechanism and properties of alkali-activated Fe-rich slags, Cem. Concr. Res. 146 (2021) 106466, https://doi.org/10.1016/j.cemconres.2021.106466.
[109] R.M. Rivera, B. Xakalashe, G. Ounoughene, K. Binnemans, B. Friedrich, T. Van Gerven, Selective rare earth element extraction using high-pressure acid leaching of slags arising from the smelting of bauxite residue, Hydrometallurgy 184 (March 2019) 162–174, https://doi.org/10.1016/j.hydromet.2019.01.005.
[110] J. Vind et al., „Rare earth element phases in bauxite residue“, Minerals, Bd. 8, Nr. 2, S. 77, Feb. 2018, doi: https://doi.org/10.3390/min8020077.
[111] J. Vind, A. Alexandri, V. Vassiliadou, und D. Panias, „Distribution of selected trace elements in the Bayer process“, Metals, Bd. 8, Nr. 5, 2018, doi: https://doi.org/10.3390/met8050327.
[112] Länderarbeitsgemeinschaft Abfall, LAGA Technische Regeln: Anforderungen an die stoffliche Verwertung von mineralischen Reststoffen/Abfällen, Zugegriffen: 7. November 2023. [Online]. Verfügbar unter: https://www.umwelt-online.de/regelwerk/cgi-bin/suchausgabe.cgi?pfad=/abfall/laga/min4.htm&such=Einbauklasse, 2023.
[113] M. Gräfe, et al., Chemistry of trace and heavy metals in bauxite residues (red mud) from Western Australia, in: Gehalten auf der 19th World Congress of Soil Science, 2010.
[114] W. Wang, Y. Pranolo, C.Y. Cheng, Recovery of scandium from synthetic red mud leach solutions by solvent extraction with D2EHPA, Sep. Purif. Technol. 108 (Apr. 2013) 96–102, https://doi.org/10.1016/j.seppur.2013.02.001.
[115] E. Lombi et al., „In situ fixation of metals in soils using bauxite residue: chemical assessment“, Environ. Pollut., Bd. 118, Nr. 3, S. 435–443, Aug. 2002, doi: https://doi.org/10.1016/S0269-7491(01)00294-9.
[116] P. Davris, E. Balomenos, D. Panias, I. Paspaliaris, Selective leaching of rare earth elements from bauxite residue (red mud), using a functionalized hydrophobic ionic liquid, Hydrometallurgy 164 (Sep. 2016) 125–135, https://doi.org/10.1016/j.hydromet.2016.06.012.
[117] F.F. Ataie, M.C.G. Juenger, S.C. Taylor-Lange, K.A. Riding, Comparison of the retarding mechanisms of zinc oxide and sucrose on cement hydration and interactions with supplementary cementitious materials, Cem. Concr. Res. 72 (2015) 128–136, https://doi.org/10.1016/j.cemconres.2015.02.023.
[118] J. Vind, et al., Modes of occurrences of scandium in Greek bauxite and bauxite residue, Miner. Eng. 123 (July 2018) 35–48, https://doi.org/10.1016/j.mineng.2018.04.025.
[119] D. A. H. Hanaor und C. C. Sorrell, „Review of the anatase to rutile phase transformation“, J. Mater. Sci., Bd. 46, Nr. 4, S. 855–874, Feb. 2011, doi: https://doi.org/10.1007/s10853-010-5113-0.
[120] L. S. Campbell, P. Henderson, F. Wall, und T. F. D. Nielsen, „Rare earth chemistry of perovskite group minerals from the Gardiner Complex, East Greenland“, Mineral. Mag., Bd. 61, Nr. 405, S. 197–212, 1997, doi: https://doi.org/10.1180/minmag.1997.061.405.04.
[121] M. Gräfe und C. Klauber, „Bauxite residue issues: IV. Old obstacles and new pathways for in situ residue bioremediation“, Hydrometallurgy, Bd. 108, Nr. 1, S. 46–59, June 2011, doi: https://doi.org/10.1016/j.hydromet.2011.02.005.

[122] M. Lee, G.M. Parkinson, P.G. Smith, F.J. Lincoln, M.M. Reyhani, Characterization of aluminum trihydroxide crystals precipitated from caustic solutions, in: Separation and Purification by Crystallization, Bd. 667, 0 Bde, ACS Symposium Series, vol. 667, American Chemical Society, 1997, pp. 123–133, https://doi.org/10.1021/bk-1997-0667.ch012, no. 667.
[123] F. R. Feret, „Selected applications of Rietveld-XRD analysis for raw materials of the aluminum industry“, Powder Diffr., Bd. 28, Nr. 2, S. 112–123, June 2013, doi: https://doi.org/10.1017/S088571561300016X.
[124] J. Vogrin, H. Hodge, T. Santini, H. Peng, J. Vaughan, Quantitative X-ray diffraction study into bauxite residue mineralogical phases, in: Gehalten auf der Light Metals 2019, Springer, 2019, pp. 93–99.
[125] H. Peng, J. Vaughan, Aluminate effect on desilication product phase transformation, J. Cryst. Growth 492 (June 2018) 84–91, https://doi.org/10.1016/j.jcrysgro.2018.04.013.
[126] T. Radomirovic, P. Smith, D. Southam, S. Tashi, F. Jones, Crystallization of sodalite particles under Bayer-type conditions, Hydrometallurgy 137 (May 2013) 84–91, https://doi.org/10.1016/j.hydromet.2013.05.006.
[127] Y. Deng, M. Flury, J. B. Harsh, A. R. Felmy, und O. Qafoku, „Cancrinite and sodalite formation in the presence of cesium, potassium, magnesium, calcium and strontium in Hanford tank waste simulants“, Appl. Geochem., Bd. 21, Nr. 12, S. 2049–2063, 2006, doi: https://doi.org/10.1016/j.apgeochem.2006.06.019.
[128] B. Xu, P. Smith, C. Wingate, und L. De Silva, „The effect of calcium and temperature on the transformation of sodalite to cancrinite in Bayer digestion“, Hydrometallurgy, Bd. 105, Nr. 1, S. 75–81, Dec. 2010, doi: https://doi.org/10.1016/j.hydromet.2010.07.010.
[129] X. Li, et al., Investigating the effect of ferrous ion on the digestion of diasporic bauxite in the Bayer process, Hydrometallurgy 152 (2015) 183–189, https://doi.org/10.1016/j.hydromet.2015.01.001.
[130] X. Pan, H. Wu, H. Yu, S. Bi, Precipitation of desilication products in CaO-$Na_2O$-$Al_2O_3$-$SiO_2$-$H_2O$ system based on the Bayer process, Hydrometallurgy 197 (2020) 105469, https://doi.org/10.1016/j.hydromet.2020.105469.
[131] J. Vogrin, T. Santini, H. Peng, J. Vaughan, The anion effect on sodium aluminosilicates formed under Bayer process digestion conditions, Hydrometallurgy 192 (2020) 105236.
[132] S. E. Dann, P. J. Mead, und M. T. Weller, „Löwenstein's rule extended to an aluminum rich framework. The structure of bicchulite, $Ca_8(Al_2SiO_6)_4(OH)_8$, by MASNMR and neutron diffraction“, Inorg. Chem., Bd. 35, Nr. 6, S. 1427–1428, 1996.
[133] B. Winkler, V. Milman, und C. Pickard, „Quantum mechanical study of Al/Si disorder in leucite and bicchulite“, Mineral. Mag., Bd. 68, Nr. 5, S. 819–824, 2004.
[134] J. Vogrin, H. Peng, T. Santini, L.J. Lee, J. Vaughan, The influence of sodium sulphate on sodium aluminosilicate solubility in Bayer liquor aiding the desilication process, Hydrometallurgy 219 (2023) 106079.
[135] J. Vogrin, T. Santini, H. Peng, J. Vaughan, Influence of chloride on sodium aluminosilicate solubility in Bayer liquor, Microporous Mesoporous Mater. 299 (2020) 110086.
[136] L. Peters, G. Vega-Flores, und W. Depmeier, „Some remarks on substitution effects in sodalites“, Prog. Solid State Chem., Bd. 37, Nr. 2, S. 243–249, 2009, doi: https://doi.org/10.1016/j.progsolidstchem.2009.11.009.
[137] V. S. Yadav, M. Prasad, J. Khan, S. Amritphale, M. Singh, und C. Raju, „Sequestration of carbon dioxide ($CO_2$) using red mud“, J. Hazard. Mater., Bd. 176, Nr. 1–3, S. 1044–1050, 2010, doi:https://doi.org/10.1016/j.jhazmat.2009.11.146.
[138] Y. Guo, X. Zhang, X. Qin, Y. Jiang, F. Zhu, S. Xue, Organic amendments enhanced the humification degree in soil formation of bauxite residue, Plant Soil (Nov. 2022), https://doi.org/10.1007/s11104-022-05773-y.
[139] G. Power, M. Gräfe, und C. Klauber, „Bauxite residue issues: I. Current management, disposal and storage practices“, Hydrometallurgy, Bd. 108, Nr. 1, S. 33–45, June 2011, doi: https://doi.org/10.1016/j.hydromet.2011.02.006.
[140] T.C. Santini, Application of the Rietveld refinement method for quantification of mineral concentrations in bauxite residues (alumina refining tailings), Int. J. Miner. Process. 139 (June 2015) 1–10, https://doi.org/10.1016/j.minpro.2015.04.004.
[141] S. Alam, S.K. Das, B.H. Rao, Characterization of coarse fraction of red mud as a civil engineering construction material, J. Clean. Prod. 168 (2017) 679–691, https://doi.org/10.1016/j.jclepro.2017.08.210.
[142] R. C. O. Romano, H. M. Bernardo, M. H. Maciel, R. G. Pileggi, und M. A. Cincotto, „Hydration of Portland cement with red mud as mineral addition“, J. Therm. Anal. Calorim., Bd. 131, Nr. 3, S. 2477–2490, March 2018, doi: https://doi.org/10.1007/s10973-017-6794-2.
[143] J. Pera, R. Boumaza, und J. Ambroise, „Development of a pozzolanic pigment from red mud“, Cem. Concr. Res., Bd. 27, Nr. 10, S. 1513–1522, Oct. 1997, doi: https://doi.org/10.1016/S0008-8846(97)00162-2.
[144] V. M. Sglavo et al., „Bauxite 'red mud' in the ceramic industry. Part 1: thermal behaviour“, J. Eur. Ceram. Soc., Bd. 20, Nr. 3, S. 235–244, März 2000, doi: https://doi.org/10.1016/S0955-2219(99)00088-6.
[145] S. Rai, K. Wasewar, und A. Agnihotri, „Treatment of alumina refinery waste (red mud) through neutralization techniques: a review“, Waste Manag. Res., Bd. 35, Nr. 6, S. 563–580, 2017.
[146] S. A. Barbhuiya, P. A. M. Basheer, M. W. Clark, und G. I. B. Rankin, „Effects of seawater-neutralised bauxite refinery residue on properties of concrete“, Cem. Concr. Compos., Bd. 33, Nr. 6, S. 668–679, July 2011, doi: https://doi.org/10.1016/j.cemconcomp.2011.03.010.
[147] R. C. Sahu, R. K. Patel, und B. C. Ray, „Neutralization of red mud using $CO_2$ sequestration cycle“, J. Hazard. Mater., Bd. 179, Nr. 1–3, S. 28–34, July 2010, doi: https://doi.org/10.1016/j.jhazmat.2010.02.052.
[148] C.J. Molineux, D.J. Newport, B. Ayati, C. Wang, S.P. Connop, J.E. Green, Bauxite residue (red mud) as a pulverised fuel ash substitute in the manufacture of lightweight aggregate, J. Clean. Prod. 112 (Jan. 2016) 401–408, https://doi.org/10.1016/j.jclepro.2015. 09.024.
[149] D. Wang, G. Chen, Z. Chen, C. Tang, Study on preparation method of strength and morphology controlled aggregates used in asphalt mixture, Constr. Build. Mater. 345 (Aug. 2022) 128189, https://doi.org/10.1016/j.conbuildmat.2022.128189.
[150] Y. Elakneswaran, et al., Characteristics of ferrite-rich Portland cement: comparison with ordinary Portland cement, Front. Mater. 6 (2019), https://doi.org/10.3389/fmats.2019.00097.
[151] D. Ariño Montoya, N. Pistofidis, G. Giannakopoulos, R. I. Iacobescu, M. S. Katsiotis, und Y. Pontikes, „Revisiting the iron-rich "ordinary Portland cement" towards valorisation of wastes: study of Fe-to-Al ratio on the clinker production and the hydration reaction“, Mater. Struct., Bd. 54, Nr. 1, S. 30, Feb. 2021, doi: https://doi.org/10.1617/s11527-020-01601-w.
[152] I. Vangelatos, G. N. Angelopoulos, und D. Boufounos, „Utilization of ferroalumina as raw material in the production of ordinary Portland cement“, J. Hazard. Mater., Bd. 168, Nr. 1, S. 473–478, Aug. 2009, doi: https://doi.org/10.1016/j.jhazmat.2009.02.049.
[153] H.F.W. Taylor, Cement Chemistry, 2nd ed., T. Telford, London, 1997.
[154] P. E. Tsakiridis, S. Agatzini-Leonardou, und P. Oustadakis, „Red mud addition in the raw meal for the production of Portland cement clinker“, J. Hazard. Mater., Bd. 116, Nr. 1, S. 103–110, Dec. 2004, doi: https://doi.org/10.1016/j.jhazmat.2004.08.002.
[155] T. Hertel, Y. Pontikes, Geopolymers, inorganic polymers, alkali-activated materials and hybrid binders from bauxite residue (red mud) — putting things in perspective, J. Clean. Prod. 258 (June 2020) S. 120610, https://doi.org/10.1016/j.jclepro.2020.120610.
[156] D. Ariño-Montoya, R. Iacobescu, G. Giannakopoulos, M. Katsiotis, Y. Pontikes, From bauxite residue to calcium sulfo-ferroaluminate cement: study of the clinkerization and hydration kynetics, in: 12ο Πανελλήνιο Επιστημονικό Συνέδριο Χημικής Μηχανικής, Athen, Mai, 2019.
[157] T. Hertel, A. Van den Bulck, S. Onisei, P.P. Sivakumar, Y. Pontikes, Boosting the use of bauxite residue (red mud) in cement — production of an Fe-rich calciumsulfoaluminate-ferrite clinker and characterisation of the hydration, Cem. Concr. Res. 145 (July 2021) 106463, https://doi.org/10.1016/j.cemconres.2021.106463.
[158] M. Singh, S. N. Upadhayay, und P. M. Prasad, „Preparation of iron rich cements using red mud“, Cem. Concr. Res., Bd. 27, Nr. 7, S. 1037–1046, 1997, doi: https://doi.org/10.1016/S0008-8846(97)00101-4.
[159] M. Singh, S. N. Upadhayay, und P. M. Prasad, „Preparation of special cements from red mud“, Waste Manag., Bd. 16, Nr. 8, S. 665–670, Jan. 1996, doi: https://doi.org/10.1016/S0956-053X(97)00004-4.
[160] Y. Jun, J. H. Kim, und T. Kim, „Hydration of calcium sulfoaluminate-based binder incorporating red mud and silica fume“, Appl. Sci., Bd. 9, Nr. 11, S. 2270, June 2019, doi: https://doi.org/10.3390/app9112270.
[161] M. Ben Haha, F. Winnefeld, A. Pisch, Advances in understanding ye'elimite-rich cements, Cement Concr. Res. 123 (Sep. 2019) 105778, https://doi.org/10.1016/j.cemconres.2019.105778.
[162] K. Ikeda, A new type of pozzolanic cement utilizing red mud and fly ash, in: Gehalten auf der 8th international congress on the chemisty of cement, 1986, pp. 389–394.
[163] K. Ikeda, Properties and possibilities of red mud cement prepared from red mud, gypsum and portlandite without clinkering process, in: Gehalten auf der International Bauxite Tailings Workshop, 1992, pp. 377–385.
[164] E.P. Manfroi, M. Cheriaf, J.C. Rocha, Microstructure, mineralogy and environmental evaluation of cementitious composites produced with red mud waste, Constr. Build. Mater. 67 (Sep. 2014) 29–36, https://doi.org/10.1016/j.conbuildmat.2013.10.031.
[165] L. Senff, D. Hotza, und J. A. Labrincha, „Effect of red mud addition on the rheological behaviour and on hardened state characteristics of cement mortars“, Constr. Build. Mater., Bd. 25, Nr. 1, S. 163–170, Jan. 2011, doi: https://doi.org/10.1016/j.conbuildmat.2010.06.043.
[166] K.S.P. Karunadasa, C.H. Manoratne, H.M.T.G.A. Pitawala, R.M.G. Rajapakse, Thermal decomposition of calcium carbonate (calcite polymorph) as examined by in-situ high-temperature X-ray powder diffraction, J. Phys. Chem. Solids 134 (Nov. 2019) 21–28, https://doi.org/10.1016/j.jpcs.2019.05.023.
[167] J. T. Kloprogge, H. D. Ruan, und R. L. Frost, „Thermal Decomposition of Bauxite Minerals: Infrared Emission Spectroscopy of Gibbsite, Boehmite and Diaspore“, S. 9.
[168] D. J. Schipper, T. W. Lathouwers, und C. Z. Doorn, „Thermal decomposition of sodalites“, J. Am. Ceram. Soc., Bd. 56, Nr. 10, S. 523–525, Oct. 1973, doi: https://doi.org/10.1111/j.1151-2916.1973.tb12402.x.
[169] L. P. Ogorodova, L. V. Mel'chakova, M. F. Vigasina, L. V. Olysich, und I. V. Pekov, „Cancrinite and cancrisilite in the Khibina-Lovozero alkaline complex: thermochemical and thermal data“, Geochem. Int., Bd. 47, Nr. 3, S. 260–267, March 2009, doi: https://doi.org/10.1134/S0016702909030045.
[170] A. Eisinas, T. Dambrauskas, K. Baltakys, und K. Ruginyte, „The peculiarities of mayenite formation from synthetic katoite and calcium monocarboaluminate samples in temperature range 25–1150 °C“, J. Therm. Anal. Calorim., Bd. 138, Nr. 3, S. 2275–2282, Nov. 2019, doi: https://doi.org/10.1007/s10973-019-08482-4.

[171] R. M. McIntosh, J. H. Sharp, und F. W. Wilburn, „The thermal decomposition of dolomite“, Thermochim. Acta, Bd. 165, Nr. 2, S. 281–296, Aug. 1990, doi: https://doi.org/10.1016/0040-6031(90)80228-Q.
[172] Z. Yang et al., „Hydration mechanisms of alkali-activated cementitious materials with ternary solid waste composition“, Materials, Bd. 15, Nr. 10, 2022, doi: https://doi.org/10.3390/ma15103616.
[173] M. Giels, T. Hertel, K. Gijbels, W. Schroeyers, Y. Pontikes, High performance mortars from vitrified bauxite residue; the quest for the optimal chemistry and processing conditions, Cement Concr. Res. 155 (May 2022) 106739, https://doi.org/10.1016/j.cemconres.2022.106739.
[174] J. Skibsted und M. D. Andersen, „The effect of alkali ions on the incorporation of aluminum in the calcium silicate hydrate (C–S–H) phase resulting from Portland cement hydration studied by $^{29}$Si MAS NMR“, J. Am. Ceram. Soc., Bd. 96, Nr. 2, S. 651–656, Feb. 2013, doi: https://doi.org/10.1111/jace.12024.
[175] D. Damidot, B. Lothenbach, D. Herfort, und F. P. Glasser, „Thermodynamics and cement science“, Cem. Concr. Res., Bd. 41, Nr. 7, S. 679–695, 2011, doi: https://doi.org/10.1016/j.cemconres.2011.03.018.
[176] B. Lothenbach, D. Damidot, T. Matschei, und J. Marchand, „Thermodynamic modelling: state of knowledge and challenges“, Adv. Cem. Res., Bd. 22, Nr. 4, S. 211–223, 2010.
[177] D. A. Kulik et al., „GEM-Selektor geochemical modeling package: revised algorithm and GEMS3K numerical kernel for coupled simulation codes“, Comput. Geosci., Bd. 17, Nr. 1, S. 1–24, Feb. 2013, doi: https://doi.org/10.1007/s10596-012-9310-6.
[178] T. Wagner, D. A. Kulik, F. F. Hingerl, und S. V. Dmytrieva, „Gem-selector geochemical modeling package: TSolMod library and data interface for multicomponent phase models“, Can. Mineral., Bd. 50, Nr. 5, S. 1173–1195, Oct. 2012, doi: https://doi.org/10.3749/canmin.50.5.1173.
[179] H. C. Helgeson und D. H. Kirkham, „Theoretical prediction of the thermodynamic behavior of aqueous electrolytes at high pressures and temperatures; II, Debye-Huckel parameters for activity coefficients and relative partial molal properties“, Am. J. Sci., Bd. 274, Nr. 10, S. 1199–1261, 1974.
[180] B. Lothenbach, E. Bernard, U. Mäder, Zeolite formation in the presence of cement hydrates and albite, Phys. Chem. Earth Pt. A/B/C 99 (2017) 77–94, https://doi.org/10.1016/j.pce.2017.02.006.
[181] T. Matschei, B. Lothenbach, und F. P. Glasser, „Thermodynamic properties of Portland cement hydrates in the system CaO–$Al_2O_3$–$SiO_2$–$CaSO_4$–$CaCO_3$–$H_2O$“, Cem. Concr. Res., Bd. 37, Nr. 10, S. 1379–1410, 2007, doi:https://doi.org/10.1016/j.cemconres.2007.06.002.
[182] B. Lothenbach und F. Winnefeld, „Thermodynamic modelling of the hydration of Portland cement“, Cem. Concr. Res., Bd. 36, Nr. 2, S. 209–226, 2006, doi:https://doi.org/10.1016/j.cemconres.2005.03.001.
[183] J. Sun, F. Zunino, K. Scrivener, Hydration and phase assemblage of limestone calcined clay cements (LC3) with clinker content below 50%, Cem. Concr. Res. 177 (2024) 107417, https://doi.org/10.1016/j.cemconres.2023.107417.
[184] B. Lothenbach, et al., Cemdata18: a chemical thermodynamic database for hydrated Portland cements and alkali-activated materials, Cem. Concr. Res. 115 (2019) 472–506, https://doi.org/10.1016/j.cemconres.2018.04.018.
[185] B. Ma, B. Lothenbach, Synthesis, characterization, and thermodynamic study of selected Na-based zeolites, Cement Concr. Res. 135 (2020) 106111, https://doi.org/10.1016/j.cemconres.2020.106111.
[186] B. Ma, B. Lothenbach, Thermodynamic study of cement/rock interactions using experimentally generated solubility data of zeolites, Cem. Concr. Res. 135 (2020) 106149, https://doi.org/10.1016/j.cemconres.2020.106149.
[187] B. Ma, B. Lothenbach, Synthesis, characterization, and thermodynamic study of selected K-based zeolites, Cem. Concr. Res. 148 (Oct. 2021) 106537, https://doi.org/10.1016/j.cemconres.2021.106537.
[188] S. Barzgar, B. Lothenbach, M. Tarik, A.D. Giacomo, C. Ludwig, The effect of sodium hydroxide on Al uptake by calcium silicate hydrates (CSH), J. Colloid Interface Sci. 572 (2020) 246–256, https://doi.org/10.1016/j.jcis.2020.03.057.
[189] I. G. Lodeiro, A. Fernández-Jimenez, A. Palomo, und D. E. Macphee, „Effect on fresh C-S-H gels of the simultaneous addition of alkali and aluminium“, Cem. Concr. Res., Bd. 40, Nr. 1, S. 27–32, 2010, doi:https://doi.org/10.1016/j.cemconres.2009.08.004.
[190] A. Kumar, G. Sant, C. Patapy, C. Gianocca, und K. L. Scrivener, „The influence of sodium and potassium hydroxide on alite hydration: experiments and simulations“, Cem. Concr. Res., Bd. 42, Nr. 11, S. 1513–1523, 2012.
[191] A. Dufresne et al., „Atomistic and mesoscale simulation of sodium and potassium adsorption in cement paste“, J. Chem. Phys., Bd. 149, Nr. 7, 2018.
[192] G. Li, P. L. Bescop, und M. Moranville, „The U phase formation in cement-based systems containing high amounts of $Na_2SO_4$“, Cem. Concr. Res., Bd. 26, Nr. 1, S. 27–33, 1996, doi:https://doi.org/10.1016/0008-8846(95)00189-1.
[193] M. Ghalehnovi, N. Roshan, A. Taghizadeh, E. Asadi Shamsabadi, S. Ali Hadigheh, und J. De Brito, „Production of environmentally friendly concrete incorporating bauxite residue and silica fume“, J. Mater. Civ. Eng., Bd. 34, Nr. 2, S. 04021423, 2022.
[194] G. Flesoura, D. Panias, A. Peys, E. Balomenos, The use of dealkalised bauxite residue in cement applications, in: TRAVAUX 52, Proceedings of the 41st International ICSOBA Conference, Dubai, Nov. 2023, pp. 951–958. Zugegriffen: 11. November 2024. [Online]. Verfügbar unter, https://icsoba.org/proceedings/41st-conference-and-exhibition-icsoba-2023/.
[195] T. Danner, M. Sletnes, und H. Justnes, „Alkali-reduced bauxite residue as novel SCM“, Nord. Concr. Res., Bd. 63, Nr. 2, S. 1–20, 2020.
[196] R.-X. Liu, C.-S. Poon, Utilization of red mud derived from bauxite in self-compacting concrete, J. Clean. Prod. 112 (2016) 384–391, https://doi.org/10.1016/j.jclepro.2015.09.049.
[197] M. Montini, X. Li, J. Rodriguez, R.G. Pileggi, K. Scrivener, Cementitious activity evaluation of bauxite residue and fly ash combination on Portland blended cement, in: TRAVAUX 48, Proceedings of the 37th International ICSOBA Conference and XXV Conference “Aluminium of Siberia”, Krasnoyarsk, Oct. 2019, pp. 491–496. Zugegriffen: 11. November 2024. [Online]. Verfügbar unter: https://icsoba.org/proceedings/37th-conference-and-exibition-icsoba-2019/.
[198] M. Putrevu, J. S. Thiyagarajan, D. Pasla, K. I. S. A. Kabeer, und K. Bisht, „Valorization of red mud waste for cleaner production of construction materials“, J. Hazard. Toxic Radioactive Waste, Bd. 25, Nr. 4, S. 03121002, Oct. 2021, doi: https://doi.org/10.1061/(ASCE)HZ.2153-5515.0000629.
[199] X. Hao, et al., In-depth insight into the cementitious synergistic effect of steel slag and red mud on the properties of composite cementitious materials, J. Build. Eng. 52 (2022) 104449.
[200] W. Zhang, et al., Synergistic enhancement of converter steelmaking slag, blast furnace slag, Bayer red mud in cementitious materials: strength, phase composition, and microstructure, J. Build. Eng. 60 (2022) 105177, https://doi.org/10.1016/j.jobe.2022.105177.
[201] B. Mota, T. Matschei, K. Scrivener, Impact of NaOH and $Na_2SO_4$ on the kinetics and microstructural development of white cement hydration, Cem. Concr. Res. 108 (June 2018) 172–185, https://doi.org/10.1016/j.cemconres.2018.03.017.
[202] B. Mota, T. Matschei, K. Scrivener, Impact of sodium gluconate on white cement-slag systems with $Na_2SO_4$, Cem. Concr. Res. 122 (2019) 59–71, https://doi.org/10.1016/j.cemconres.2019.04.008.
[203] M. Zhang, F. Zunino, L. Yang, F. Wang, K. Scrivener, Understanding the negative effects of alkalis on long-term strength of Portland cement, Cem. Concr. Res. 174 (2023) 107348, https://doi.org/10.1016/j.cemconres.2023.107348.
[204] R. Rathan Raj, J. Brijitta, D. Ramachandran, E.B. Perumal Pillai, Microstructure evolution in ordinary Portland cement–metakaolin–red mud-based ternary blended cement, J. Inst. Eng. (India) Ser. A 100 (2019) 707–718.
[205] V. Jobbágy, J. Somlai, J. Kovács, G. Szeiler, und T. Kovács, „Dependence of radon emanation of red mud bauxite processing wastes on heat treatment“, J. Hazard. Mater., Bd. 172, Nr. 2, S. 1258–1263, Dec. 2009, doi: https://doi.org/10.1016/j.jhazmat.2009.07.131.
[206] X. Liu, N. Zhang, H. Sun, J. Zhang, und L. Li, „Structural investigation relating to the cementitious activity of bauxite residue — red mud“, Cem. Concr. Res., Bd. 41, Nr. 8, S. 847–853, Aug. 2011, doi: https://doi.org/10.1016/j.cemconres.2011.04.004.
[207] L. Zhou, M. Gou, W. Hou, M. Zhao, J. Zhao, und Z. Shen, „Effect of thermal activation and particle size on cementitious activity of bauxite tailings“, Environ. Sci. Pollut. Res., Bd. 29, Nr. 52, S. 78960–78972, 2022.
[208] H. Chen, H. Sun, H. Li, Effect of heat treatment temperature on cementitious activity of red mud, Light Met. 9 (2006) 22–25.
[209] N. Ye, J. Zhu, J. Liu, Y. Li, X. Ke, J. Yang, Influence of thermal treatment on phase transformation and dissolubility of aluminosilicate phase in red mud, MRS Proc. 1488 (2012), https://doi.org/10.1557/opl.2012.1546. S. imrc12-1488-7b-055.
[210] T. Hertel, B. Blanpain, Y. Pontikes, High temperature processing options for the valorisation of bauxite residue towards new materials, in: Gehalten auf der Proceedings of 35th International ICSOBA Conference, 2017.
[211] T. Hertel, A. Van den Bulck, B. Blanpain, Y. Pontikes, An integrated process for iron recovery and binder production from bauxite residue (red mud), Mater. Lett. 264 (Apr. 2020) 127273, https://doi.org/10.1016/j.matlet.2019.127273.
[212] S. Srikanth, A. K. Ray, A. Bandopadhyay, B. Ravikumar, und A. Jha, „Phase constitution during sintering of red mud and red mud–fly ash mixtures“, J. Am. Ceram. Soc., Bd. 88, Nr. 9, S. 2396–2401, Sep. 2005, doi: https://doi.org/10.1111/j.1551-2916.2005.00471.x.
[213] A. Alujas, R. Fernández, R. Quintana, K.L. Scrivener, F. Martirena, Pozzolanic reactivity of low grade kaolinitic clays: influence of calcination temperature and impact of calcination products on OPC hydration, Appl. Clay Sci. 108 (2015) 94–101, https://doi.org/10.1016/j.clay.2015.01.028.
[214] F. Bullerjahn, M. Zajac, J. Pekarkova, D. Nied, Novel SCM produced by the co-calcination of aluminosilicates with dolomite, Cem. Concr. Res. 134 (2020) 106083, https://doi.org/10.1016/j.cemconres.2020.106083.
[215] C. R. Borra, B. Blanpain, Y. Pontikes, K. Binnemans, und T. Van Gerven, „Smelting of bauxite residue (red mud) in view of iron and selective rare earths recovery“, J. Sustain. Metall., Bd. 2, Nr. 1, S. 28–37, March 2016, doi: https://doi.org/10.1007/s40831-015-0026-4.
[216] X. Li, T. Zhang, K. Wang, G. Lv, X. Chao, und X. Yang, „Experimental research on vortex melting reduction of high-iron red mud (bauxite residue)“, Bull. Environ. Contam. Toxicol., Bd. 109, Nr. 1, S. 155–162, July 2022, doi: https://doi.org/10.1007/s00128-022-03501-x.
[217] A. Lazou, C. Van Der Eijk, K. Tang, E. Balomenos, L. Kolbeinsen, und J. Safarian, „The utilization of bauxite residue with a calcite-rich bauxite ore in the Pedersen process for iron and alumina extraction“, Metall. Mater. Trans. B Process Metall. Mater. Process. Sci., Bd. 52, Nr. 3, S. 1255–1266, June 2021, doi: https://doi.org/10.1007/s11663-021-02086-w.
[218] M. S. Archambo und S. K. Kawatra, „Utilization of bauxite residue: recovering iron values using the iron nugget process“, Miner. Process. Extr. Metall. Rev., Bd. 42, Nr. 4, S. 222–230, 2021, doi: https://doi.org/10.1080/08827508.2020.1720982.
[219] M. Vafeias, A. Bempelou, E. Georgala, P. Davris, E. Balomenos, und D. Panias, „Leaching of Ca-rich slags produced from reductive smelting of bauxite residue with $Na_2CO_3$ solutions for alumina extraction: lab and pilot scale experiments“, Minerals, Bd. 11, Nr. 8, 2021, doi: https://doi.org/10.3390/min11080896.
[220] F. Bullerjahn, M. Mehringskötter, Synthetic granulated blast furnace-like slag from bauxite residue smelting and its use in multi-component Portland composite

cement, J. Clean. Prod. 329 (Dec. 2021) 129667, https://doi.org/10.1016/j.jclepro.2021.129667.
[221] D. Londono-Zuluaga et al., „Report of RILEM TC 267-TRM phase 3: validation of the R3 reactivity test across a wide range of materials“, Mater. Struct., Bd. 55, Nr. 5, S. 142, May 2022, doi: https://doi.org/10.1617/s11527-022-01947-3.
[222] X. Zhu, T. Zhang, und G. Lü, „Kinetics of carbonated decomposition of hydrogarnet with different silica saturation coefficients“, Int. J. Miner. Metall. Mater., Bd. 27, Nr. 4, S. 472–482, Apr. 2020, doi: https://doi.org/10.1007/s12613-019-1913-7.
[223] M. Zajac, J. Skibsted, F. Bullerjahn, J. Skocek, Semi-dry carbonation of recycled concrete paste, J. CO2 Util. 63 (Sep. 2022) 102111, https://doi.org/10.1016/j.jcou.2022.102111.
[224] Y. Wang, T. Zhang, G. Lv, Y. Liu, W. Zhang, Q. Zhao, Overview of process control of novel calcification-carbonation process for bauxite residue treatment, Hydrometallurgy 199 (2021) 105536.
[225] S. Khaitan, D. A. Dzombak, und G. V. Lowry, „Mechanisms of neutralization of bauxite residue by carbon dioxide“, J. Environ. Eng., Bd. 135, Nr. 6, S. 433–438, 2009.
[226] X. Kong, et al., Natural evolution of alkaline characteristics in bauxite residue, J. Clean. Prod. 143 (2017) 224–230, https://doi.org/10.1016/j.jclepro.2016.12.125.
[227] D. J. Cooling, P. S. Hay, und L. Guilfoyle, „Carbonation of bauxite resdiue“, in Proceedings of the 6th International Alumina Quality Workshop, Brisbane: AQW Inc., S. 185–190.
[228] N. Zhang, H. Sun, X. Liu, und J. Zhang, „Early-age characteristics of red mud–coal gangue cementitious material“, J. Hazard. Mater., Bd. 167, Nr. 1–3, S. 927–932, Aug. 2009, doi: https://doi.org/10.1016/j.jhazmat.2009.01.086.
[229] Düsseldorf, Dekarbonisierung von Zement und Beton — Minderungspfade und Handlungsstrategien, review. [Online]. Verfügbar unter: https://www.vdz-online.de/dekarbonisierung, 2020.
[230] Cembuerau, „Cementing the European Green Deal — reaching climate neutrality along the cement and concrete value chain by 2050“, Cembuereau the European Cement Association, Brussels, Positionspapier/Pressemitteilung. Zugegriffen: 17. Februar 2022. [Online]. Verfügbar unter: https://cembureau.eu/library/.
[231] J. Zhang, et al., Sustainable utilization of bauxite residue (Red Mud) as a road material in pavements: a critical review, Constr. Build. Mater. 270 (Feb. 2021) 121419, https://doi.org/10.1016/j.conbuildmat.2020.121419.
[232] C. Venkatesh, N. Ruben, und M. S. R. Chand, „Red mud as an additive in concrete: comprehensive characterization“, J. Korean Ceram. Soc., Bd. 57, Nr. 3, S. 281–289, May 2020, doi: https://doi.org/10.1007/s43207-020-00030-3.
[233] R. C. de Oliveira Romano, C. C. Liberato, J. Borges Gallo, M. Montini, M. A. Cincotto, und R. G. Pileggi, „Evaluation of transition from fluid to elastic solid of cementitious pastes with bauxite residue using oscillation rheometry and isothermal calorimetry“, Appl. Rheol., Bd. 2, Nr. 23, S. 23822–9, 2013, doi: https://doi.org/10.3933/APPLRHEOL-23-23830.
[234] A.L. Fujii, D. dos Reis Torres, R.C. de Oliveira Romano, M.A. Cincotto, R. G. Pileggi, Impact of superplasticizer on the hardening of slag Portland cement blended with red mud, Construct. Build. Mater. 101 (Dec. 2015) 432–439, https://doi.org/10.1016/j.conbuild-mat.2015.10.057.
[235] M. Giels, T. Hertel, M. Sommerfeld, C. Dertmann, B. Friedrich, und Y. Pontikes, „BR09-Optimizing the Potential of BR Slag in Blended Cement“.
[236] J. Zhang, N. Zhang, J. Yuan, J. Zhao, J. Zhang, und Y. Zhang, „Mortar designed from red mud with iron tailings and moulded by 3D printing“, Bull. Environ. Contam. Toxicol., Bd. 109, Nr. 1, S. 95–100, 2022.
[237] D. V. Ribeiro, J. A. Labrincha, und M. R. Morelli, „Chloride diffusivity in red mud-ordinary Portland cement concrete determined by migration tests“, Mater. Res., Bd. 14, Nr. 2, S. 227–234, May 2011, doi: https://doi.org/10.1590/S1516-14392011005000026.
[238] W.C. Tang, Z. Wang, S.W. Donne, M. Forghani, Y. Liu, Influence of red mud on mechanical and durability performance of self-compacting concrete, J. Hazard. Mater. 379 (2019) 120802, https://doi.org/10.1016/j.jhazmat.2019.120802.
[239] T. Hertel, S. Onisei, P.P. Sivakumar, Y. Pontikes, Pozzolanic activity of thermally treated bauxite residue in blends with ordinary portland cement, in: Gehalten auf der Proceedings of the 5th International Slag Valorisation Symposium, 2017, pp. 267–270.
[240] K. Ganesan, K. Rajagopal, und K. Thangavel, „Evaluation of bagasse ash as supplementary cementitious material“, Cem. Concr. Compos., Bd. 29, Nr. 6, S. 515–524, July 2007, doi: https://doi.org/10.1016/j.cemconcomp.2007.03.001.
[241] N. Chusilp, C. Jaturapitakkul, und K. Kiattikomol, „Effects of LOI of ground bagasse ash on the compressive strength and sulfate resistance of mortars“, Constr. Build. Mater., Bd. 23, Nr. 12, S. 3523–3531, Dec. 2009, doi: https://doi.org/10.1016/j.conbuildmat.2009.06.046.
[242] S. Praveenkumar, G. Sankarasubramanian, S. Sindhu, Strength, permeability and microstructure characterization of pulverized bagasse ash in cement mortars, Construct. Build. Mater. 238 (March 2020) 117691, https://doi.org/10.1016/j.conbuildmat.2019.117691.
[243] H. Maraghechi, F. Avet, H. Wong, H. Kamyab, und K. Scrivener, „Performance of Limestone Calcined Clay Cement (LC3) with various kaolinite contents with respect to chloride transport“, Mater. Struct., Bd. 51, Nr. 5, S. 1–17, 2018.
[244] T. Danner und H. Justnes, „Bauxite residue as supplementary cementitious material — efforts to reduce the amount of soluble sodium“, Nord. Concr. Res., Bd. 62, Nr. 1, S. 1–20, June 2020, doi: https://doi.org/10.2478/ncr-2020-0001.
[245] N. Smaoui, M. A. Bérubé, B. Fournier, B. Bissonnette, und B. Durand, „Effects of alkali addition on the mechanical properties and durability of concrete“, Cem. Concr. Res., Bd. 35, Nr. 2, S. 203–212, 2005, doi:https://doi.org/10.1016/j.cemconres.2004.05.007.
[246] S. Barzgar, B. Lothenbach, M. Tarik, A.D. Giacomo, C. Ludwig, The effect of sodium hydroxide on Al uptake by calcium silicate hydrates (CSH), J. Colloid Interface Sci. 572 (2020) 246–256, https://doi.org/10.1016/j.jcis.2020.03.057.
[247] E. L'Hôpital, B. Lothenbach, K. Scrivener, D.A. Kulik, Alkali uptake in calcium alumina silicate hydrate (C-A-S-H), Cem. Concr. Res. 85 (2016) 122–136, https://doi.org/10.1016/j.cemconres.2016.03.009.
[248] L. Tang, Study of the Possibilities of Using Red Mud as an Additive in Concrete and Grout Mortar, Svensk Kärnbränslehantering AB Swedish Nuclear Fuel and Waste Management Co., Stockholm, Sweden, 2014.
[249] R. Liu, C. Poon, Effects of red mud on properties of self-compacting mortar, J. Clean. Prod. 135 (Nov. 2016) 1170–1178, https://doi.org/10.1016/j.jclepro.2016.07.052.
[250] M. Ghalehnovi, E. Asadi Shamsabadi, A. Khodabakhshian, F. Sourmeh, J. de Brito, Self-compacting architectural concrete production using red mud, Constr. Build. Mater. 226 (Nov. 2019) 418–427, https://doi.org/10.1016/j.conbuildmat.2019.07.248.
[251] M. Ghalehnovi, N. Roshan, E. Hakak, E.A. Shamsabadi, J. de Brito, Effect of red mud (bauxite residue) as cement replacement on the properties of self-compacting concrete incorporating various fillers, J. Clean. Prod. 240 (2019) 118213, https://doi.org/10.1016/j.jclepro.2019.118213.
[252] M.U. Salim, M.A. Mosaberpanah, A. Danish, N. Ahmad, R.A. Khalid, C. Moro, Role of bauxite residue as a binding material and its effect on engineering properties of cementitious composites: a review, Constr. Build. Mater. 409 (2023) 133844, https://doi.org/10.1016/j.conbuildmat.2023.133844.
[253] L. M. V. Silveira, M. H. Maciel, J. A. F. S. Mesquita, M. A. Cincotto, R. C. O. Romano, und R. G. Pileggi, „Hydration and chemical shrinkage of Portland cement with bauxite residue from Bayer process“, J. Therm. Anal. Calorim., Bd. 148, Nr. 14, S. 6715–6729, July 2023, doi: https://doi.org/10.1007/s10973-023-12201-5.
[254] W. Yodsudjai, K. Wang, Chemical shrinkage behavior of pastes made with different types of cements, Constr. Build. Mater. 40 (2013) 854–862, https://doi.org/10.1016/j.conbuildmat.2012.11.053.
[255] F. Rajabipour, G. Sant, und J. Weiss, „Interactions between shrinkage reducing admixtures (SRA) and cement paste's pore solution“, Cem. Concr. Res., Bd. 38, Nr. 5, S. 606–615, 2008, doi:https://doi.org/10.1016/j.cemconres.2007.12.005.
[256] A. Bayat, H. Rooholamini, und M. M. B. Farahani, „Effect of bauxite residue inclusion on the strength, shrinkage, and abrasion of alkali-activated slag concrete“, Innov. Infrastruct. Solut., Bd. 7, Nr. 6, S. 331, Sep. 2022, doi: https://doi.org/10.1007/s41062-022-00932-7.
[257] A. Bayat, A. Hassani, A.A. Yousefi, Effects of red mud on the properties of fresh and hardened alkali-activated slag paste and mortar, Constr. Build. Mater. 167 (2018) 775–790, https://doi.org/10.1016/j.conbuildmat.2018.02.105.
[258] G. A. Rao, „Long-term drying shrinkage of mortar — influence of silica fume and size of fine aggregate“, Cem. Concr. Res., Bd. 31, Nr. 2, S. 171–175, Feb. 2001, doi: https://doi.org/10.1016/S0008-8846(00)00347-1.
[259] K. Viyasun, R. Anuradha, K. Thangapandi, D.S. Kumar, A. Sivakrishna, R. Gobinath, Investigation on performance of red mud based concrete, Mater. Today Proc. 39 (2021) 796–799.
[260] M. Anirudh, K.S. Rekha, C. Venkatesh, R. Nerella, Characterization of red mud based cement mortar; mechanical and microstructure studies, Mater. Today Proc. 43 (2021) 1587–1591.
[261] R. R. Raja, E. Pillaib, und A. Santhakumarc, „Effective utilization of redmud bauxite waste as a re-placement of cement in concrete for environmental conservation“, Ecol. Environ. Conserv., Bd. 19, Nr. 1, S. 247–255, 2013.
[262] S. von Greve-Dierfeld et al., „Understanding the carbonation of concrete with supplementary cementitious materials: a critical review by RILEM TC 281-CCC“, Mater. Struct., Bd. 53, Nr. 6, S. 136, Dec. 2020, doi: https://doi.org/10.1617/s11527-020-01558-w.
[263] U. Raghu Babu und B. Kondraivendhan, „Influence of bauxite residue (red mud) on corrosion of rebar in concrete“, Innov. Infrastruct. Solut., Bd. 5, Nr. 3, S. 108, Dec. 2020, doi: https://doi.org/10.1007/s41062-020-00356-1.
[264] C. Venkatesh, R. Nerella, M.S.R. Chand, Comparison of mechanical and durability properties of treated and untreated red mud concrete, Mater. Today Proc. 27 (2020) 284–287.
[265] B. S. Dhanya und M. Santhanam, „Performance evaluation of rapid chloride permeability test in concretes with supplementary cementitious materials“, Mater. Struct., Bd. 50, Nr. 1, S. 67, Aug. 2016, doi: https://doi.org/10.1617/s11527-016-0940-3.
[266] K.D. Weerdt, W. Wilson, A. Machner, F. Georget, Chloride profiles — what do they tell us and how should they be used? Cem. Concr. Res. 173 (2023) 107287, https://doi.org/10.1016/j.cemconres.2023.107287.
[267] C. Rodriguez-Navarro, E. Doehne, und E. Sebastian, „How does sodium sulfate crystallize? Implications for the decay and testing of building materials“, Cem. Concr. Res., Bd. 30, Nr. 10, S. 1527–1534, 2000, doi:https://doi.org/10.1016/S0008-8846(00)00381-1.
[268] Q. Wang, W. Wilson, K. Scrivener, Unidirectional Sulfate Ingress in Limestone Calcined Clay Cement (LC3) Pastes Under Cyclic Exposure, 2021.
[269] J. Bizzozero, C. Gosselin, K.L. Scrivener, Expansion mechanisms in calcium aluminate and sulfoaluminate systems with calcium sulfate, Cem. Concr. Res. 56 (2014) 190–202, https://doi.org/10.1016/j.cemconres.2013.11.011.
[270] D. P. Bentz, „Influence of alkalis on porosity percolation in hydrating cement pastes“, Cem. Concr. Compos., Bd. 28, Nr. 5, S. 427–431, 2006, doi:https://doi.org/10.1016/j.cemconcomp.2006.01.003.
[271] M. Thomas, „The effect of supplementary cementing materials on alkali-silica reaction: a review“, Cem. Concr. Res., Bd. 41, Nr. 12, S. 1224–1231, 2011, doi: https://doi.org/10.1016/j.cemconres.2010.11.003.

[272] J. Moraes Neves, M.S. Rebmann, R.C.O. Romano, R.G. Pileggi, The effects of bauxite residue on the alkali silica reaction in cementitious composites, in: L.F. M. Sanchez, C. Trottier (Eds.), Proceedings of the 17th International Conference on Alkali-Aggregate Reaction in Concrete, Springer Nature Switzerland, Cham, 2024, pp. 643–649.
[273] S.-Y. Hong und F. Glasser, „Alkali binding in cement pastes: part I. The CSH phase“, Cem. Concr. Res., Bd. 29, Nr. 12, S. 1893–1903, 1999.
[274] T. Chappex und K. Scrivener, „Alkali fixation of C–S–H in blended cement pastes and its relation to alkali silica reaction“, Cem. Concr. Res., Bd. 42, Nr. 8, S. 1049–1054, Aug. 2012, doi: https://doi.org/10.1016/j.cemconres.2012.03.010.
[275] M. Bhatty, N. Greening, Interaction of alkalies with hydrating and hydrated calcium silicates, in: Gehalten auf der Proceedings, 1978, pp. 87–112.